

---

# Simplifying Momentum-based Riemannian Submanifold Optimization

---

Wu Lin<sup>1</sup> Valentin Duruisseaux<sup>2</sup> Melvin Leok<sup>2</sup>  
 Frank Nielsen<sup>3</sup> Mohammad Emtiyaz Khan<sup>4</sup> Mark Schmidt<sup>1,5</sup>

## Abstract

Riemannian submanifold optimization with momentum is computationally challenging because ensuring iterates remain on the submanifold often requires solving difficult differential equations. We simplify such optimization algorithms for the submanifold of symmetric positive-definite matrices with the affine invariant metric. We propose a generalized version of the Riemannian normal coordinates which dynamically trivializes the problem into a Euclidean unconstrained problem. We use our approach to explain and simplify existing approaches for structured covariances and develop efficient second-order optimizers for deep learning without explicit matrix inverses.

## 1. Introduction

Symmetric positive definite (SPD) estimation plays an essential role in machine learning. For example, optimization methods such as adaptive gradient methods and Newton’s method require estimating a SPD preconditioner. In Gaussian variational inference, a learned SPD covariance matrix serves as a posterior approximation. Other cases include dictionary learning (Cherian & Sra, 2016), trace regression (Slawski et al., 2015) for kernel matrices, metric learning (Guillaumin et al., 2009), log-det maximization (Wang et al., 2010), Gaussian mixtures (Hosseini & Sra, 2015), and Gaussian graphical models (Makam et al., 2021).

Riemannian gradient descent (RGD) can be helpful for SPD matrix estimation since the set of SPD matrices forms a Riemannian manifold. However, this can be computationally infeasible in high-dimensions due to manifold operations that involve full-rank matrix inverses (see Table 1). A natural choice is to consider a sparse SPD matrix, which introduces additional constraints. In principle, Riemannian approaches can be applied when the set of constraint-satisfying SPD

matrices forms a submanifold. Unfortunately, most manifold operations needed for Riemannian optimization are either computationally intractable or unknown. For example, the Riemannian gradient computation may involve another matrix inversion (see Table 1). Other operations such as the Riemannian exponential map and the parallel transport map are defined by solving an intractable matrix ordinary differential equation (ODE).

Using moving coordinates is an attractive idea to develop practical Riemannian methods, where a local coordinate is generated, used, and discarded at each iteration. Traditionally, a global coordinate that specifies the constraints is used in the literature. Existing Riemannian momentum methods are studied in a given global coordinate system and require approximate solutions of matrix ODEs in these coordinates. However, using global coordinates increases the computational intensity of approximating the matrix ODEs needed for manifold optimization, as they involve computing nonsparse and high-order derivatives of a matrix, which limits the large-scale usage of Riemannian methods. On the contrary, local coordinates such as the ones suggested by structured natural-gradient descent (NGD) (Lin et al., 2021a) have been demonstrated to efficiently handle constraints on structured Gaussian distributions in a Bayesian context. However, it is unclear how to incorporate momentum in a computationally efficient way with respect to these moving coordinates, while also taking a given Riemannian metric into consideration.

We propose special local coordinates for a class of SPD submanifolds with the affine invariant metric to avoid the use of global coordinates, and of the exact Riemannian exponential and transport maps that are required by existing Riemannian momentum methods, and instead exploit sparse matrix structures to obtain an efficient update scheme. Under our local coordinates, all constraints disappear and the Riemannian metric at evaluation points becomes the standard Euclidean metric. This trivialization enables an efficient Riemannian momentum update by performing the standard (Euclidean) gradient descent with momentum update in the local coordinates. We extend structured NGD by establishing its connection to Riemannian methods (Sec. 3.1), demystifying the construction of existing local coordinates (Sec. 3.2), introducing our new coordinates for efficient momentum computation (Sec. 3.1), and expanding the scope to struc-

---

<sup>1</sup>University of British Columbia. <sup>2</sup>University of California San Diego <sup>3</sup>Sony Computer Science Laboratories Inc. <sup>4</sup>RIKEN Center for Advanced Intelligence Project. <sup>5</sup>CIFAR AI Chair, Alberta Machine Intelligence Institute. Correspondence to: Wu Lin <yorker.lin@gmail.com >.

tured SPD matrices without Gaussian and Bayesian assumptions (Sec. 3.3). Finally, we develop inverse-free structured matrix optimizers for deep learning (Sec. 4).

## 2. Manifold Optimization and its Challenges

Consider a complete manifold  $\mathcal{M}$  with a Riemannian metric  $\mathbf{F}$  represented by a single global coordinate  $\tau$ . Under this coordinate system, Riemannian gradient descent (Absil et al., 2009; Bonnabel, 2013) (RGD) is defined as

$$\text{RGD} : \tau \leftarrow \text{RExp}(\tau, -\beta \mathbf{F}^{-1}(\tau) \mathbf{g}(\tau)), \quad (1)$$

where  $\mathbf{v}(\tau) := \mathbf{F}^{-1}(\tau) \mathbf{g}(\tau)$  is a Riemannian gradient,  $\mathbf{g}(\tau)$  is a Euclidean gradient,  $\mathbf{F}$  is the metric,  $\beta$  is a step-size, and  $\text{RExp}(\tau, \mathbf{v})$  is the Riemannian exponential map defined by solving a nonlinear (geodesic) ODE (see Appx. C.3). The nonlinearity of the ODE makes it difficult to obtain a closed-form expression for the solution.

To incorporate momentum in RGD, a Riemannian parallel transport map  $\hat{T}_{\tau^{(\text{cur})} \rightarrow \tau^{(\text{new})}}(\mathbf{v}^{(\text{cur})})$  is introduced to move the Riemannian vector  $\mathbf{v}^{(\text{cur})}$  computed at the current point  $\tau^{(\text{cur})}$  to a new point  $\tau^{(\text{new})}$  on the manifold. Alimisis et al. (2020) propose a Riemannian momentum method using the Riemannian transport map (see Appx. C.4). We consider an equivalent update (shown in Appx. C.6) by using a Euclidean transport map (defined in Appx. C.5)  $T_{\tau^{(\text{cur})} \rightarrow \tau^{(\text{new})}}(\mathbf{m}^{(\text{cur})})$  to move a Euclidean vector  $\mathbf{m}^{(\text{cur})}$ :

$$\begin{aligned} \text{Momentum} : \mathbf{m}^{(\text{cur})} &\leftarrow \alpha \mathbf{w}^{(\text{cur})} + \beta \mathbf{g}(\tau^{(\text{cur})}), \\ \text{RGD} : \tau^{(\text{new})} &\leftarrow \text{RExp}(\tau^{(\text{cur})}, -\mathbf{F}^{-1}(\tau^{(\text{cur})}) \mathbf{m}^{(\text{cur})}), \\ \text{Transport} : \mathbf{w}^{(\text{new})} &\leftarrow T_{\tau^{(\text{cur})} \rightarrow \tau^{(\text{new})}}(\mathbf{m}^{(\text{cur})}), \end{aligned} \quad (2)$$

for step-size  $\beta$  and momentum weight  $\alpha$ . The use of the Euclidean map is essential for efficient approximations of transport maps as will be discussed in Sec. 3.1. Both transport maps are defined by solving transport ODEs (Appx. C.4-C.5). However, solving any of the ODEs can be computationally intensive since it is a linear system of differential equations and the solution involves matrix decomposition.

### 2.1. Challenges in SPD Manifold and Submanifolds

Consider a  $k$ -by- $k$  SPD manifold  $\mathcal{M} = \{\tau \in \mathbb{R}^{k \times k} \mid \tau \succ 0\}$ . The affine invariant metric  $\mathbf{F}$  for the SPD manifold (see Theorem 2.10 of Minh & Murino (2017)) is defined as twice the Fisher-Rao metric (see Appx. C.1) for the  $k$ -dimensional Gaussian distribution  $\mathcal{N}(\mathbf{0}, \tau)$  with zero mean and covariance  $\tau$ , which is the 2nd derivative of a matrix,

$$\mathbf{F}(\tau) = -2 \mathbb{E}_{\mathcal{N}(\mathbf{0}, \tau)} [\nabla_{\tau}^2 \log \mathcal{N}(\mathbf{0}, \tau)]. \quad (3)$$

In the SPD manifold case, the Riemannian maps (see Table 1) have a closed-form expression. However, both updates in Eq. (1) and Eq. (2) require computing full-rank matrix inverse in the Riemannian maps, so such methods

are impractical in high-dimensional cases. We will propose an alternative approach to construct practical Riemannian methods for SPD submanifolds in higher-dimensions.

For many SPD submanifolds with the same (induced) metric, it is nontrivial to implement updates in both Eq. (1) and Eq. (2) since these needed Riemannian maps do not admit a closed-form expression. For example, consider the following SPD submanifold, which can be used (Calvo & Oller, 1990) to represent a  $(k-1)$ -dimensional Gaussian with mean  $\boldsymbol{\mu}$  and covariance  $\boldsymbol{\Sigma} := \mathbf{V} - \boldsymbol{\mu} \boldsymbol{\mu}^T$ ,

$$\mathcal{M} = \left\{ \tau = \begin{bmatrix} \mathbf{V} & \boldsymbol{\mu} \\ \boldsymbol{\mu}^T & 1 \end{bmatrix} \in \mathbb{R}^{k \times k} \mid \tau \succ 0 \right\}.$$

In this case, it is an open problem to find the closed-form expression of the Riemannian exponential map. The Riemannian exponential map is also unknown on other SPD submanifolds such as the rank-one SPD submanifold,

$$\mathcal{M} = \left\{ \tau = \begin{bmatrix} a^2 & ab^T \\ ab & \mathbf{b} \mathbf{b}^T + \text{Diag}(c^2) \end{bmatrix} \in \mathbb{R}^{k \times k} \mid \tau \succ 0 \right\}.$$

The existing Riemannian maps defined on the full SPD manifold cannot be used on SPD submanifolds since these maps do not persevere the submanifold structures, and in particular, do not guarantee that their output stays on a given SPD submanifold. For an approximation of the Riemannian maps, we often have to evaluate the ODEs. However, it is computationally challenging to even evaluate the ODEs at a point when the global coordinate  $\tau$  is used, since this requires computing the Christoffel symbols  $\Gamma_{cb}^a(\tau)$  (defined in Appx. C.2) arising in the ODEs. These symbols are defined by partial derivatives of the metric  $\mathbf{F}(\tau)$  in Eq. (3), so their computation involves complicated 3rd order derivatives of a matrix. Furthermore, it is unclear how to efficiently compute a Riemannian gradient  $\mathbf{F}^{-1}(\tau) \mathbf{g}(\tau)$  on a SPD submanifold without explicitly inverting the metric, which can be another computationally intensive operation.

### 2.2. Natural-gradient Descent and its Challenges

A practical approach is natural-gradient descent (NGD), which approximates the Riemannian exponential map by ignoring the Christoffel symbols. A NGD update is a linear approximation of the update of Eq. (1) given by

$$\tau \leftarrow \tau - \beta \mathbf{F}^{-1}(\tau) \mathbf{g}(\tau). \quad (4)$$

This update is also known as the Euclidean retraction map (Jeuris et al., 2012). Unfortunately, NGD in the global coordinate  $\tau$  does not guarantee that the update stays on a manifold even in the full SPD case. Moreover, computing Riemannian gradients remains challenging due to the metric inversion. Structured NGD (Lin et al., 2021a) addressed the SPD constraint of Gaussians in variational Bayesian settings by performing NGD on local coordinates. Local coordinates could enable efficient Riemannian gradient computation by

Operations on SPD in global $\tau$	Manifold	Submanifolds
Riemann. gradient $\mathbf{v}$ at $\tau_0$	$\tau_0 \mathbf{g} \tau_0$	$\mathbf{F}^{-1}(\tau_0) \mathbf{g}$
Riemann. exponential $\text{RExp}(\tau_0, \mathbf{v})$	$\tau_0^{1/2} \text{Exp}(\tau_0^{-1/2} \mathbf{v} \tau_0^{-1/2}) \tau_0^{1/2}$	Unknown
Riemann. transport $\hat{T}_{\tau_0 \rightarrow \tau_1}(\mathbf{v})$	$\mathbf{E} \mathbf{v} \mathbf{E}^T$ ; $\mathbf{E} := (\tau_1 \tau_0^{-1})^{1/2}$	Unknown
Euclidean transport $T_{\tau_0 \rightarrow \tau_1}(\mathbf{g})$	$\mathbf{H} \mathbf{g} \mathbf{H}^T$ ; $\mathbf{H} := \tau_1^{-1} \mathbf{E} \tau_0$	Unknown

Table 1. Manifold operations compatible with affine invariant metric  $\mathbf{F}$ , where  $\text{Exp}(\mathbf{N}) = \sum_{k=0}^{\infty} \frac{1}{k!} \mathbf{N}^k$  is the matrix exponential function, and  $\mathbf{g}$  is a (symmetric) Euclidean gradient at  $\tau_0$ . On submanifolds,  $\tau$  denotes learnable parameters.

simplifying the metric inversion computation. However, it is nontrivial to incorporate momentum in structured NGD due to the metric and the use of moving coordinates. We address this issue and develop practical Riemannian momentum methods by using generalized normal coordinates. Using our normal coordinates, we will explain and generalize structured NGD from a deterministic manifold perspective. We further expand the scope of structured NGD to SPD submanifolds by going beyond the Bayesian settings.

### 2.3. Standard Normal Coordinates

**Defn 1:** A metric  $\mathbf{F}$  is trivialized at  $\eta_0 = \mathbf{0}$  if  $\mathbf{F}(\eta_0) = \mathbf{I}$ , where  $\mathbf{I}$  is the identity matrix.

Normal coordinates are used to simplify calculations in differential geometry and general relativity. However, normal coordinates are seldom studied in the optimization literature. Given a reference point  $\tau^{(\text{cur})}$ , the Riemannian normal (local) coordinate  $\eta$  at  $\tau^{(\text{cur})}$  is defined as below, where  $\tau^{(\text{cur})}$  and  $\mathbf{F}^{-1/2}(\tau^{(\text{cur})})$  are treated as constants in coordinate  $\eta$ .

$$\tau = \psi_{\tau^{(\text{cur})}}(\eta) := \text{RExp}(\tau^{(\text{cur})}, \mathbf{F}^{-1/2}(\tau^{(\text{cur})}) \eta). \quad (5)$$

$\mathbf{F}^{-1/2}(\tau^{(\text{cur})})$  in Eq. (5) is essential since it trivializes the metric at  $\eta_0$  and will simplify the Riemannian gradient computation in Eq. (6) and Eq. (8). Lezcano (2019; 2020) considered non-Riemannian normal coordinates defined by the Riemannian exponential map such as  $\tau = \text{RExp}(\tau^{(\text{cur})}, \lambda)$ . However, the metric is neither trivialized (i.e.,  $\mathbf{F}(\lambda_0) = \mathbf{F}(\tau^{(\text{cur})})$  at  $\lambda_0 = \mathbf{0}$ ) nor incorporated into their coordinates for efficient computation and approximations.

A Riemannian normal coordinate has nice computational properties, summarized in Table 2. In coordinate  $\eta$ , the origin  $\eta_0 := \mathbf{0}$  represents the point  $\tau^{(\text{cur})} = \psi_{\tau^{(\text{cur})}}(\eta_0)$ .

RGD in Eq. (1) can be reexpressed as (Euclidean) gradient descent (GD) in local coordinate  $\eta$  since the metric  $\mathbf{F}(\eta_0)$  at  $\eta_0$  becomes the standard Euclidean metric  $\mathbf{I}$ :

$$\begin{aligned} \text{GD} : \eta_1 &\leftarrow \eta_0 - \beta \mathbf{F}^{-1}(\eta_0) \mathbf{g}(\eta_0) = -\beta \mathbf{g}(\eta_0), \\ \tau^{(\text{new})} &\leftarrow \psi_{\tau^{(\text{cur})}}(\eta_1), \end{aligned} \quad (6)$$

where  $\mathbf{g}(\eta_0) = \mathbf{F}^{-1/2}(\tau^{(\text{cur})}) \mathbf{g}(\tau^{(\text{cur})})$  is a Euclidean gradient evaluated at  $\eta_0$ . Since the metric  $\mathbf{F}(\eta_0)$  is trivialized, the GD update is also a NGD update in coordinate  $\eta$ . The trivialization of the metric makes it easy to add momentum

	Standard Coordinate	Generalized Coordinate
$\tau$	$\psi_{\tau^{(\text{cur})}}(\eta)$	$\phi_{\tau^{(\text{cur})}}(\eta)$
$\tau^{(\text{cur})}$	$\psi_{\tau^{(\text{cur})}}(\eta_0)$	$\phi_{\tau^{(\text{cur})}}(\eta_0)$
$\mathbf{F}(\eta_0)$	$\mathbf{I}$	$\mathbf{I}$
$\Gamma_{bc}^a(\eta_0)$	0	can be nonzero

Table 2. Properties of Riemannian normal coordinates  $\eta$  defined at  $\tau^{(\text{cur})}$ , where the original  $\eta_0 = \mathbf{0}$  represents  $\tau^{(\text{cur})}$ ,  $\psi$  is defined by the Riemannian exponential map, and  $\phi$  is a diffeomorphic map

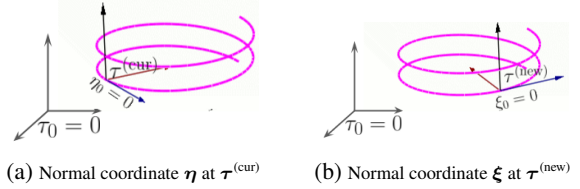


Figure 1. Normal coordinates are generated at each iteration

into RGD while taking the metric into consideration.

In the SPD case,  $\mathbf{F}^{-1/2}(\tau) \eta = \tau^{1/2} \eta \tau^{1/2}$ , where  $\eta$  is a symmetric matrix. The metric  $\mathbf{F}(\eta)$  is trivialized at  $\eta_0$  as

$$\mathbf{F}(\eta_0) = -2 \mathbb{E}_{\mathcal{N}(\mathbf{0}, \tau)} [\nabla_{\eta}^2 \log \mathcal{N}(\mathbf{0}, \tau)] \Big|_{\eta=\eta_0} = \mathbf{I},$$

where  $\tau = \psi_{\tau^{(\text{cur})}}(\eta)$ . By Table 1, the normal coordinate admits a closed-form, where  $\eta$  is symmetric and  $\tau$  is SPD,

$$\psi_{\tau^{(\text{cur})}}(\eta) = (\tau^{(\text{cur})})^{1/2} \text{Exp}(\eta) (\tau^{(\text{cur})})^{1/2}. \quad (7)$$

Note that we do not obtain Eq. (7) using coordinates in Lezcano (2019; 2020) due to the missing term  $\mathbf{F}^{-1/2}(\tau^{(\text{cur})})$ .

In the case of SPD submanifolds, it is hard to use the standard Riemannian normal coordinate as it relies on the intractable Riemannian exponential map, as seen in Eq. (5). However, we will generalize the normal coordinate in Eq. (7) for a SPD manifold to SPD submanifolds.

## 3. Generalized Normal Coordinates

We propose new normal coordinates to simplify the momentum computation on a class of SPD submanifolds. Inspired by the standard normal coordinates, we identify their properties that enable efficient Riemannian optimization, and generalize normal coordinates by defining new coordinates satisfying these properties on a general (sub)manifold.

**Defn 2:** A local coordinate is a generalized Riemannian normal coordinate at a reference point  $\tau^{(\text{cur})}$  denoted by  $\tau = \phi_{\tau^{(\text{cur})}}(\eta)$  if  $\phi_{\tau^{(\text{cur})}}(\eta)$  satisfies all the following assumptions.

**Assumption 1:** The origin  $\eta_0 = \mathbf{0}$  represents the reference point  $\tau^{(\text{cur})} = \phi_{\tau^{(\text{cur})}}(\eta_0)$  in coordinate  $\eta$ .

**Assumption 2:** The metric  $\mathbf{F}(\eta_0) = \mathbf{I}$  is trivialized at  $\eta_0$ .

**Assumption 3:** The map  $\phi_{\tau^{(\text{cur})}}(\eta)$  is bijective.  $\phi_{\tau^{(\text{cur})}}$  and  $\phi_{\tau^{(\text{cur})}}^{-1}$  are smooth (i.e.  $\phi_{\tau^{(\text{cur})}}(\eta)$  is diffeomorphic).

**Assumption 4:** The parameter space of  $\eta$  is a vector space.

Assumption 1 enables simplification using the chain rule of high-order derivative calculations (i.e., the metric and Christoffel symbols in Appx. E and F) by evaluating at zero, which is useful when computing Christoffel symbols. Assumption 2 enables metric preservation in GD updates by dynamically trivializing the metric. By Assumption 3, (sub)manifold constraints disappear in these coordinates, and Assumption 4 ensures that scalar products and vector additions are well-defined, so that we can perform GD. The standard normal coordinates satisfy Assumption 1-2 shown in Table 2. Assumption 3 is satisfied due to the Riemannian exponential map. On a complete manifold, the normal coordinate also satisfies Assumption 4 (Absil et al., 2009). These assumptions make it easy to design new normal coordinates without computing the Riemannian exponential map. Thus, both the affine invariant metric and the (sub)manifold constraints are trivialized in our coordinates. Our approach is different from Lezcano (2019; 2020); Lin et al. (2021a;b), where the metric is not trivialized in their coordinates.

We will design our coordinates to work with NGD/GD by satisfying Assumptions 1-4 while reducing the computational cost by ignoring Christoffel symbols (see Table 2). A standard GD update using our coordinates is an approximation of the exact RGD update in Eq. (6). As will be shown in Sec. 3.3.1, this GD resembles structured NGD in Gaussian cases, both of which ignore Christoffel symbols,

$$\begin{aligned} \text{GD} : \boldsymbol{\eta}_1 &\leftarrow \boldsymbol{\eta}_0 - \beta \mathbf{F}^{-1}(\boldsymbol{\eta}_0) \mathbf{g}(\boldsymbol{\eta}_0) = -\beta \mathbf{g}(\boldsymbol{\eta}_0), \\ \boldsymbol{\tau}^{(\text{new})} &\leftarrow \phi_{\boldsymbol{\tau}^{(\text{cur})}}(\boldsymbol{\eta}_1). \end{aligned}$$

### 3.1. Adding Momentum using Normal Coordinates

Since the metric is trivialized at  $\boldsymbol{\eta}_0$ , we propose simply adding (Euclidean) momentum in the GD update in our normal coordinates. At each iteration, given the current point  $\boldsymbol{\tau}^{(\text{cur})}$  in the global coordinate, we generate a normal coordinate  $\boldsymbol{\eta}$  at  $\boldsymbol{\tau}^{(\text{cur})}$  and perform the update in coordinate  $\boldsymbol{\eta}$ , where we first assume momentum  $\mathbf{w}^{(\boldsymbol{\eta}_0)}$  is given.

$$\begin{aligned} \text{Momentum} : \mathbf{m}^{(\boldsymbol{\eta}_0)} &\leftarrow \alpha \mathbf{w}^{(\boldsymbol{\eta}_0)} + \beta \mathbf{g}(\boldsymbol{\eta}_0), \\ \text{GD} : \boldsymbol{\eta}_1 &\leftarrow \boldsymbol{\eta}_0 - \mathbf{F}^{-1}(\boldsymbol{\eta}_0) \mathbf{m}^{(\boldsymbol{\eta}_0)} = -\mathbf{m}^{(\boldsymbol{\eta}_0)}, \\ \boldsymbol{\tau}^{(\text{new})} &\leftarrow \phi_{\boldsymbol{\tau}^{(\text{cur})}}(\boldsymbol{\eta}_1), \end{aligned} \quad (8)$$

where  $\alpha$  is the momentum weight and  $\beta$  is the step-size.

We now discuss how to include momentum in moving coordinates  $\boldsymbol{\eta}$  and  $\boldsymbol{\xi}$ , where  $\boldsymbol{\eta}$  and  $\boldsymbol{\xi}$  are normal coordinates defined at  $\boldsymbol{\tau}^{(\text{cur})}$  and  $\boldsymbol{\tau}^{(\text{new})}$ , respectively. Note that  $\boldsymbol{\tau}^{(\text{new})}$  is represented by  $\boldsymbol{\eta}_1$  in current coordinate  $\boldsymbol{\eta}$  and by  $\boldsymbol{\xi}_0$  in new coordinate  $\boldsymbol{\xi}$ . To compute  $\mathbf{w}^{(\boldsymbol{\xi}_0)}$  in coordinate  $\boldsymbol{\xi}$  at the next iteration, we perform the following two steps.

**Step 1: (In Coordinate  $\boldsymbol{\eta}$ )** We transport momentum  $\mathbf{m}^{(\boldsymbol{\eta}_0)}$  at point  $\boldsymbol{\tau}^{(\text{cur})}$  via the Euclidean transport map to point  $\boldsymbol{\tau}^{(\text{new})}$ , which is similar to the transport step in Eq. (2).

Since performing NGD/GD alone ignores Christoffel symbols, we suggest ignoring the symbols in the approximation

of the transport map  $T_{\boldsymbol{\eta}_0 \rightarrow \boldsymbol{\eta}_1}(\mathbf{m}^{(\boldsymbol{\eta}_0)})$  using coordinate  $\boldsymbol{\eta}$ . This gives the following update:

$$\text{Transport} : \mathbf{w}^{(\boldsymbol{\eta}_1)} \leftarrow \mathbf{m}^{(\boldsymbol{\eta}_0)}. \quad (9)$$

The approximation keeps the dominant term of the map and ignores negligible terms. This approximation is known as the Euclidean vector transport map (Jeuris et al., 2012) and the vector-transport-free map (Godaz et al., 2021). A similar approximation is also suggested in Riemannian sampling (Giolami & Calderhead, 2011) to avoid solving an implicit leapfrog update. Using our coordinates, we can make a better approximation by adding the second dominant term (see Appx. F) defined by the symbols. For example, in SPD cases, the second dominant term (see Eq. (35) in Appx. F) can be explicitly computed and is negligible compared to the first term. The computation can be similarly carried out in submanifold cases. Moreover, if our normal coordinate  $\boldsymbol{\eta}$  is a symmetric matrix as will be shown in Eq. (11), the second dominant term vanishes even for the non-vanishing Christoffel symbols. On the other hand, it can be non-trivial to compute the second term under a global coordinate  $\boldsymbol{\tau}$ .

**Step 2: (At Point  $\boldsymbol{\tau}^{(\text{new})}$ )** We coordinate-transform momentum  $\mathbf{w}^{(\boldsymbol{\eta}_1)}$  from coordinate  $\boldsymbol{\eta}$  to coordinate  $\boldsymbol{\xi}$  and return the transformation as  $\mathbf{w}^{(\boldsymbol{\xi}_0)}$ , where  $\boldsymbol{\eta}_1$  and  $\boldsymbol{\xi}_0$  represent  $\boldsymbol{\tau}^{(\text{new})}$ .

By construction of the normal coordinates (shown in Fig. 1), coordinates  $\boldsymbol{\eta}$  and  $\boldsymbol{\xi}$  represent the global coordinate  $\boldsymbol{\tau}$  as  $\boldsymbol{\tau} = \phi_{\boldsymbol{\tau}^{(\text{cur})}}(\boldsymbol{\eta}) = \phi_{\boldsymbol{\tau}^{(\text{new})}}(\boldsymbol{\xi})$ , where  $\boldsymbol{\xi}$  is the normal coordinate associated to  $\boldsymbol{\tau}^{(\text{new})}$  at the next iteration. We transform momentum  $\mathbf{w}^{(\boldsymbol{\eta}_1)}$  as a Euclidean (gradient) vector from coordinate  $\boldsymbol{\eta}$  to coordinate  $\boldsymbol{\xi}$  via the (Euclidean) chain rule,

$$\left(\mathbf{w}^{(\boldsymbol{\xi}_0)}\right)^T = \left(\mathbf{w}^{(\boldsymbol{\eta}_1)}\right)^T \mathbf{J}(\boldsymbol{\xi}_0); \quad \mathbf{J}(\boldsymbol{\xi}) := \frac{\partial \boldsymbol{\eta}}{\partial \boldsymbol{\xi}}, \quad (10)$$

where  $\boldsymbol{\xi}_0 = \mathbf{0}$ ,  $\boldsymbol{\eta} = \phi_{\boldsymbol{\tau}^{(\text{cur})}}^{-1} \circ \phi_{\boldsymbol{\tau}^{(\text{new})}}(\boldsymbol{\xi})$ , and  $\mathbf{J}(\boldsymbol{\xi})$  is the Jacobian. Thanks to our coordinates, the Jacobian computation can be simplified by evaluating at  $\boldsymbol{\xi}_0 = \mathbf{0}$ .

We can see that our update in Eq. (8)-(10) is a practical approximation of update (2). The Euclidean transport map is required for the use of the (Euclidean) chain rule and simplification of the Jacobian computation in Eq. (10).

### 3.2. Designing Our Coordinates for SPD Manifolds

We describe how to design generalized normal coordinates on SPD manifolds. This procedure explains the construction of existing local coordinates in structured NGD.

To mimic the standard normal coordinate in Eq. (7), consider the matrix factorization  $\boldsymbol{\tau}^{(\text{cur})} = \mathbf{A}^{(\text{cur})} \left(\mathbf{A}^{(\text{cur})}\right)^T$ , where  $\mathbf{A}$  is invertible (not a Cholesky). This is an asymmetric square root factorization, which is different from the symmetric version in Eq. (7). The non-vanishing Christoffel symbols appear due to the asymmetric factorization. This factorization allows us to obtain the following local coordinate by approximating the standard coordinate  $\boldsymbol{\psi}_{\boldsymbol{\tau}^{(\text{cur})}}$  as

$$\begin{aligned}\phi_{\tau^{(\text{cur})}}(\boldsymbol{\eta}) &:= \mathbf{A}^{(\text{cur})} \text{Exp}_{\text{m}}(\boldsymbol{\eta}) \left( \mathbf{A}^{(\text{cur})} \right)^T \\ &= \mathbf{A}^{(\text{cur})} \text{Exp}_{\text{m}}\left(\frac{1}{2}\boldsymbol{\eta}\right) \text{Exp}_{\text{m}}^T\left(\frac{1}{2}\boldsymbol{\eta}\right) \left( \mathbf{A}^{(\text{cur})} \right)^T = \mathbf{A} \mathbf{A}^T, \quad (11)\end{aligned}$$

where  $\mathbf{A} := \mathbf{A}^{(\text{cur})} \text{Exp}_{\text{m}}\left(\frac{1}{2}\boldsymbol{\eta}\right)$  and  $\boldsymbol{\eta}$  is a symmetric matrix. Factorization  $\boldsymbol{\tau} = \mathbf{A} \mathbf{A}^T$  can be non-unique since we work in coordinate  $\boldsymbol{\eta}$  instead of coordinate  $\mathbf{A}$ . To satisfy injectivity/uniqueness in  $\boldsymbol{\eta}$  as required by Assumption 3, we restrict  $\boldsymbol{\eta}$  to be in a subspace of  $\mathbb{R}^{k \times k}$  such as the symmetric matrix space. We can show that  $\boldsymbol{\eta}$  is a generalized normal coordinate at  $\boldsymbol{\tau}^{(\text{cur})}$  (see Appx. H.1). Using other factorizations, we obtain more generalized coordinates:

- $\phi_{\tau^{(\text{cur})}}(\boldsymbol{\eta}) = \mathbf{B}^{-T} \mathbf{B}^{-1}$ , with  $\mathbf{B} := \mathbf{B}^{(\text{cur})} \text{Exp}_{\text{m}}\left(-\frac{1}{2}\boldsymbol{\eta}\right)$
- $\phi_{\tau^{(\text{cur})}}(\boldsymbol{\eta}) = \mathbf{C}^T \mathbf{C}$ , with  $\mathbf{C} := \text{Exp}_{\text{m}}\left(\frac{1}{2}\boldsymbol{\eta}\right) \mathbf{C}^{(\text{cur})}$

where  $\boldsymbol{\eta}$  is a symmetric matrix in both cases. For (unique) Cholesky factor  $\mathbf{A}$ , we obtain a new coordinate by restricting  $\boldsymbol{\eta}$  to be a lower-triangular matrix with proper scaling.

The normal coordinate considered in Eq. (11) is similar to local coordinates in structured NGD, where  $\mathbf{A}$  is referred to as an auxiliary coordinate. The authors of structured NGD (Lin et al., 2021a) introduced a similar local coordinate as  $\mathbf{A} := \mathbf{A}^{(\text{cur})} \text{Exp}_{\text{m}}(\boldsymbol{\eta})$  in Gaussian cases without providing the construction and mentioning other local coordinates. The metric is not trivialized in their local coordinates. Our procedure sheds light on the construction and the role of local coordinates in structured NGD. For example, our construction explains why  $\mathbf{A} = \mathbf{A}^{(\text{cur})} \text{Exp}_{\text{m}}(\boldsymbol{\eta})$  instead of  $\mathbf{A} = \text{Exp}_{\text{m}}(\boldsymbol{\eta}) \mathbf{A}^{(\text{cur})}$  is used in structured NGD for the factorization  $\boldsymbol{\tau} = \mathbf{A} \mathbf{A}^T$ . Using  $\mathbf{A} = \text{Exp}_{\text{m}}(\boldsymbol{\eta}) \mathbf{A}^{(\text{cur})}$  in structured NGD makes it difficult to compute natural-gradients since the metric is not trivialized. On the contrary, our coordinates explicitly trivialize the metric, which makes it easy to compute (natural) gradients and include momentum.

Using the normal coordinate in Eq. (11), our update in Eq. (8)-(10) can be simplified as shown in Appx. H.3.

Godaz et al. (2021) consider a special case for a full SPD manifold with symmetric  $\boldsymbol{\eta}$  and a unique factor  $\mathbf{A}$ . Their vector-transport-free update is exactly our approximation in Eq. (9). However, their method is non-constructive. Our constructive approach generalizes their method by allowing  $\boldsymbol{\eta}$  to be an asymmetric matrix, using a non-unique factor  $\mathbf{A}$ , and extending their method to SPD submanifolds.

### 3.3. Designing Our Coordinates for SPD Submanifolds

Although the standard normal coordinates are unknown on SPD submanifolds, our generalized normal coordinates allow us to work on a class of SPD submanifolds by noting that  $\mathbf{A}$  is in the general linear group  $\text{GL}^{k \times k}$  known as a Lie group. Matrix structures are preserved under matrix multiplication and the matrix exponential function. The coordinate space of  $\boldsymbol{\eta}$  is a (vector) subspace of the tangent space of  $\text{Exp}_{\text{m}}(\boldsymbol{\eta})$  at  $\mathbf{I}$  known as the Lie algebra of  $\text{GL}^{k \times k}$ .

Thus, Assumption 4 is satisfied. These observations allow us to consider the following class of SPD submanifolds:

$$\mathcal{M} = \left\{ \boldsymbol{\tau} = \mathbf{A} \mathbf{A}^T \in \mathbb{R}^{k \times k} \mid \mathbf{A} \in \text{a subgroup of } \text{GL}^{k \times k} \right\}.$$

We give two examples of SPD submanifolds, where we construct the corresponding normal coordinates. In Sec. 3.3.1, we present our update without the Bayesian and Gaussian assumptions. Our update recovers structured NGD as a special case by making a Gaussian assumption. In Sec. 3.3.2, we demonstrate the scalability of our update maps.

#### 3.3.1. GAUSSIAN FAMILY AS A SPD SUBMANIFOLD

We will first consider a SPD submanifold in a non-Bayesian and non-Gaussian setting. We then show how our update relates to structured NGD in Gaussian cases where Gaussian gradient identities are available. Consider the SPD submanifold, where  $\succ$  denotes the SPD constraint,

$$\mathcal{M} = \left\{ \boldsymbol{\tau} = \begin{bmatrix} \mathbf{V} & \boldsymbol{\mu} \\ \boldsymbol{\mu}^T & 1 \end{bmatrix} \in \mathbb{R}^{(d+1) \times (d+1)} \mid \boldsymbol{\tau} \succ 0 \right\}.$$

Note that  $\boldsymbol{\tau}^{-1} = \begin{bmatrix} \boldsymbol{\Sigma}^{-1} & -\boldsymbol{\Sigma}^{-1} \boldsymbol{\mu} \\ -\boldsymbol{\mu}^T \boldsymbol{\Sigma}^{-1} & 1 + \boldsymbol{\mu}^T \boldsymbol{\Sigma}^{-1} \boldsymbol{\mu} \end{bmatrix}$ , for  $\boldsymbol{\tau} \in \mathcal{M}$  and  $\boldsymbol{\Sigma} := \mathbf{V} - \boldsymbol{\mu} \boldsymbol{\mu}^T$ . Thus,  $\boldsymbol{\Sigma} \succ 0$  since  $\boldsymbol{\tau}^{-1} \succ 0$ . Then, letting  $\boldsymbol{\Sigma} = \mathbf{L} \mathbf{L}^T$ ,  $\mathcal{M}$  can be reexpressed as

$$\mathcal{M} = \left\{ \boldsymbol{\tau} = \mathbf{A} \mathbf{A}^T \mid \mathbf{A} := \begin{bmatrix} \mathbf{L} & \boldsymbol{\mu} \\ \mathbf{0} & 1 \end{bmatrix}, \mathbf{L} \in \text{GL}^{d \times d} \right\}.$$

Observe that  $\mathbf{A}$  is in a subgroup of  $\text{GL}^{(d+1) \times (d+1)}$ . We construct a normal coordinate  $\phi_{\tau^{(\text{cur})}}(\boldsymbol{\eta}) = \mathbf{A} \mathbf{A}^T$  similar to the one in Eq. (11), where

$$\mathbf{A} = \mathbf{A}^{(\text{cur})} \text{Exp}_{\text{m}} \left( \begin{bmatrix} \frac{1}{2} \boldsymbol{\eta}_L & \frac{1}{\sqrt{2}} \boldsymbol{\eta}_\mu \\ \mathbf{0} & 0 \end{bmatrix} \right), \quad (12)$$

and  $\boldsymbol{\eta} = \{\boldsymbol{\eta}_L, \boldsymbol{\eta}_\mu\}$ ,  $\boldsymbol{\eta}_L \in \mathbb{R}^{d \times d}$  is a symmetric matrix so that Assumption 3 is satisfied. The scalars highlighted in red are needed for Assumption 2 so that the metric is trivialized.

There is another normal coordinate  $\phi_{\tau^{(\text{cur})}}(\boldsymbol{\eta}) = \mathbf{A} \mathbf{A}^T$  when

$$\begin{aligned}\mathbf{A} &= \mathbf{A}^{(\text{cur})} \begin{bmatrix} \text{Exp}_{\text{m}}\left(\frac{1}{2}\boldsymbol{\eta}_L\right) & \frac{1}{\sqrt{2}}\boldsymbol{\eta}_\mu \\ \mathbf{0} & 1 \end{bmatrix} \\ &= \begin{bmatrix} \mathbf{L}^{(\text{cur})} \text{Exp}_{\text{m}}\left(\frac{1}{2}\boldsymbol{\eta}_L\right) & \boldsymbol{\mu}^{(\text{cur})} + \frac{1}{\sqrt{2}} \mathbf{L}^{(\text{cur})} \boldsymbol{\eta}_\mu \\ \mathbf{0} & 1 \end{bmatrix}. \quad (13)\end{aligned}$$

We can obtain Eq. (13) from Eq. (12) (shown in Appx. G.1).

Using the normal coordinate in either Eq. (12) or Eq. (13), the Euclidean gradient needed in Eq. (8) is given by

$$\mathbf{g}(\boldsymbol{\eta}_0) = \{\mathbf{L}^T \mathbf{g}_1 \mathbf{L}, \sqrt{2} \mathbf{L}^T (\mathbf{g}_1 \boldsymbol{\mu} + \mathbf{g}_2)\},$$

where  $\mathbf{L} = \mathbf{L}^{(\text{cur})}$ ,  $\boldsymbol{\mu} = \boldsymbol{\mu}^{(\text{cur})}$ ,  $\mathbf{g}(\boldsymbol{\tau}^{(\text{cur})}) = \begin{bmatrix} \mathbf{g}_1 & \mathbf{g}_2 \\ \mathbf{g}_2^T & 0 \end{bmatrix}$  is a (symmetric) Euclidean gradient w.r.t.  $\boldsymbol{\tau} \in \mathcal{M}$ . The vector-Jacobian product in Eq. (10) is easy to compute by using coordinate Eq. (13). Note that the computation of this product depends on the choice of normal coordinates.

Our update can be used for SPD estimation such as metric learning, trace regression, and dictionary learning from a deterministic matrix manifold optimization perspective. Neither Bayesian nor Gaussian assumptions are required.

In Gaussian cases, Calvo & Oller (1990) show that a  $d$ -dimensional Gaussian  $\mathcal{N}(\mathbf{z}|\boldsymbol{\mu}, \boldsymbol{\Sigma})$  with mean  $\boldsymbol{\mu}$  and covariance  $\boldsymbol{\Sigma}$  can be reexpressed as an augmented  $(d+1)$ -dimensional Gaussian  $\mathcal{N}(\mathbf{x}|\mathbf{0}, \boldsymbol{\tau})$  with zero mean and covariance  $\boldsymbol{\tau}$ , where  $\mathbf{x}^T = [\mathbf{z}^T, 1]$  and  $\boldsymbol{\tau}$  is on this SPD submanifold. Hosseini & Sra (2015) considered this reparametrization for maximum likelihood estimation (MLE) of Gaussian mixture models, but their method is only guaranteed to converge to this particular submanifold at the optimum as they use the Riemannian maps for the corresponding full SPD manifold. On the contrary, our update not only stays on this SPD submanifold at each iteration but is also applicable to other SPD submanifolds. Our approach expands the scope of structured NGD originally proposed as a Bayesian estimator to a maximum likelihood estimator for Gaussian mixture models with *structured covariances* where existing methods such as Hosseini & Sra (2015) and the expectation-maximization algorithm cannot be applied.

We now show that structured NGD is a special case of our update. The update of structured NGD (Lin et al., 2021a) for Gaussian  $\mathcal{N}(\boldsymbol{\mu}, \boldsymbol{\Sigma})$  with the Fisher-Rao metric is

$$\boldsymbol{\mu} \leftarrow \boldsymbol{\mu} - \gamma \boldsymbol{\Sigma} \mathbf{g}_\mu, \quad \mathbf{L} \leftarrow \mathbf{L} \text{Exp}(\!-\gamma \mathbf{L}^T \mathbf{g}_\Sigma \mathbf{L}), \quad (14)$$

where  $\boldsymbol{\Sigma} = \mathbf{L}\mathbf{L}^T$  and  $\gamma$  is the step-size for structured NGD.

As shown in Appx. G.2, we can reexpress  $\mathbf{g}_1$  and  $\mathbf{g}_2$  using Gaussian gradients  $\mathbf{g}_\mu$  and  $\mathbf{g}_\Sigma$  as  $\mathbf{g}_1 = \mathbf{g}_\Sigma$  and  $\mathbf{g}_2 = \frac{1}{2}(\mathbf{g}_\mu - 2\mathbf{g}_\Sigma \boldsymbol{\mu})$ . Thus, we reexpress  $\mathbf{g}(\boldsymbol{\eta}_0)$  as

$$\mathbf{g}(\boldsymbol{\eta}_0) = \{\mathbf{L}^T \mathbf{g}_\Sigma \mathbf{L}, \frac{1}{\sqrt{2}} \mathbf{L}^T \mathbf{g}_\mu\}. \quad (15)$$

Since the affine invariant metric is twice the Fisher-Rao metric (see Eq. (3)), we set step-size  $\beta = 2\gamma$  and momentum weight  $\alpha = 0$ . Our update (without momentum) in Eq. (8) recovers structured NGD in Eq. (14) by using the Gaussian gradients in Eq. (15) and coordinate (13).

Using coordinate (13), our update essentially performs NGD in the expectation parameter space  $\{\boldsymbol{\mu}, \boldsymbol{\Sigma} + \boldsymbol{\mu}\boldsymbol{\mu}^T\}$  of a Gaussian by considering the Gaussian as an exponential family. Likewise, using another coordinate such as  $\boldsymbol{\tau} = \mathbf{B}^{-T} \mathbf{B}^{-1}$ , our update performs NGD in the natural parameter space  $\{-\boldsymbol{\Sigma}^{-1} \boldsymbol{\mu}, \boldsymbol{\Sigma}^{-1}\}$ , which is a dual space of the expectation parameter space (Khan & Lin, 2017).

### 3.3.2. RANK-ONE SPD SUBMANIFOLD

Now, we give an example of sparse SPD matrices to illustrate the usage of our update in high-dimensional problems.

Consider the following SPD submanifold,

$$\mathcal{M} = \left\{ \boldsymbol{\tau} = \begin{bmatrix} a^2 & ab^T \\ ab & \mathbf{b}\mathbf{b}^T + \text{Diag}(\mathbf{c}^2) \end{bmatrix} \in \mathbb{R}^{(d+1) \times (d+1)} \mid \boldsymbol{\tau} \succ 0 \right\}.$$

To use our normal coordinates, we reexpress  $\mathcal{M}$  as

$$\mathcal{M} = \left\{ \boldsymbol{\tau} = \mathbf{A}\mathbf{A}^T \mid \mathbf{A} := \begin{bmatrix} a & \mathbf{0} \\ \mathbf{b} & \text{Diag}(\mathbf{c}) \end{bmatrix}, a > 0, \mathbf{c} > 0 \right\},$$

where  $\text{Diag}(\mathbf{c})$  is in the diagonal subgroup of  $\text{GL}^{d \times d}$ . Observe that  $\mathbf{A}$  is in a subgroup of  $\text{GL}^{(d+1) \times (d+1)}$ . Thus, we can construct the following generalized normal coordinate,

$$\boldsymbol{\tau} = \mathbf{A}\mathbf{A}^T; \quad \mathbf{A} = \mathbf{A}^{(\text{cur})} \text{Exp}(\mathbf{D} \odot \boldsymbol{\eta}),$$

where  $\boldsymbol{\eta} = \begin{bmatrix} \eta_a & \mathbf{0} \\ \boldsymbol{\eta}_b & \text{Diag}(\boldsymbol{\eta}_c) \end{bmatrix} \in \mathbb{R}^{(d+1) \times (d+1)}$ ,  $\odot$  is the elementwise product, and the constant matrix  $\mathbf{D} = \frac{1}{2} \begin{bmatrix} 1 & \mathbf{0} \\ \sqrt{2}\mathbf{1} & \mathbf{I} \end{bmatrix}$  enforces Assumption 2, with  $\mathbf{1}$  denoting a matrix of ones.

Similarly, we can compute Euclidean gradient Eq. (8) as

$$\mathbf{g}(\boldsymbol{\eta}_0) = \begin{bmatrix} a(ag_1 + 2\mathbf{g}_2^T \mathbf{b}) + \mathbf{b}^T \mathbf{f} & \mathbf{0} \\ \sqrt{2}\mathbf{c} \odot (ag_2 + \mathbf{f}) & \text{Diag}(\mathbf{c}^2 \odot \text{diag}(\mathbf{G}_3)) \end{bmatrix},$$

where  $\mathbf{f} = \mathbf{G}_3 \mathbf{b}$  and  $\mathbf{g}(\boldsymbol{\tau}^{(\text{cur})}) = \begin{bmatrix} g_1 & \mathbf{g}_2^T \\ \mathbf{g}_2 & \mathbf{G}_3 \end{bmatrix}$  is a (symmetric) Euclidean gradient w.r.t.  $\boldsymbol{\tau}$ . The computation of Eq. (10) can be found in Appx. D.

If we can directly compute  $\mathbf{f} = \mathbf{G}_3 \mathbf{b}$  and  $\text{diag}(\mathbf{G}_3)$  without computing  $\mathbf{G}_3$ , it is easy to scale up our update (8) to high-dimensional settings, by truncating the matrix exponential function as  $\text{Exp}(\mathbf{N}) \approx \mathbf{I} + \mathbf{N} + \frac{1}{2}\mathbf{N}^2$ . This truncation preserves the matrix structure and non-singularity of  $\mathbf{A}$ .

## 4. Generalization for Deep Learning

In this section, we propose inverse-free structured matrix optimizers for deep learning.

To solve a minimization problem  $\min_{\boldsymbol{\mu} \in \mathbb{R}^k} \ell(\boldsymbol{\mu})$ , Lin et al. (2021b) proposed using structured NGD as preconditioned gradient descent with a SPD preconditioner  $\mathbf{S} := \mathbf{B}\mathbf{B}^T$ ,

$$\boldsymbol{\mu} \leftarrow \boldsymbol{\mu} - \beta \mathbf{S}^{-1} \mathbf{g}_\mu, \quad \mathbf{B} \leftarrow \mathbf{B} \text{Exp}(\!-\frac{\beta}{2} \mathbf{B}^{-1} \mathbf{g}_\Sigma \mathbf{B}^{-T}), \quad (16)$$

where  $\mathbf{g}_\Sigma := \frac{1}{2}(\nabla_\mu^2 \ell(\boldsymbol{\mu}) - \mathbf{S})$ , and  $\mathbf{g}_\mu := \nabla_\mu \ell(\boldsymbol{\mu})$ . This update requires a matrix inverse which can be slow and numerically unstable in large-scale NN training due to the use of low-precision floating-point training schemes.

We can show that Eq. (16) is obtained by considering the inverse of the preconditioner  $\boldsymbol{\tau} = \mathbf{S}^{-1} = \mathbf{B}^{-T} \mathbf{B}^{-1}$  as a SPD manifold. The update of  $\mathbf{B}$  can be obtained by using our normal coordinate in Sec. 3.2 as  $\boldsymbol{\tau} = \mathbf{B}^{-T} \mathbf{B}^{-1}$  where  $\mathbf{B} = \mathbf{B}^{(\text{cur})} \text{Exp}(\!-\frac{1}{2} \boldsymbol{\eta})$ . As shown in Eq. (43) in Appx. H.3, the minus sign is canceled out by another minus sign in the GD update of Eq. (8).

We can obtain a matrix-inverse-free update (see Appx. H.3):

$$\boldsymbol{\mu} \leftarrow \boldsymbol{\mu} - \beta \mathbf{A}\mathbf{A}^T \mathbf{g}_\mu, \quad (17)$$

Our Matrix-inverse-free Update	KFAC Optimizer
1: At Frequency $T$ , update $\mathbf{m}_K, \mathbf{m}_C, \mathbf{K}, \mathbf{C}$ Obtain $\boldsymbol{\mu}_{AA} \otimes \boldsymbol{\mu}_{GG}$ to approximate $\nabla_{\boldsymbol{\mu}}^2 \ell(\boldsymbol{\mu})$ $\mathbf{m}_K \leftarrow \alpha_1 \mathbf{m}_K + \frac{\beta_1}{2d} (\text{Tr}(\mathbf{H}_C) \mathbf{H}_K + c^2 \mathbf{K}^T \mathbf{K} - d \mathbf{I}_p)$ $\mathbf{m}_C \leftarrow \alpha_1 \mathbf{m}_C + \frac{\beta_1}{2p} (\text{Tr}(\mathbf{H}_K) \mathbf{H}_C + k^2 \mathbf{C}^T \mathbf{C} - p \mathbf{I}_d)$ $\mathbf{K} \leftarrow \mathbf{K} \text{Exp}m(-\mathbf{m}_K) \approx \mathbf{K}(\mathbf{I}_p - \mathbf{m}_K)$ $\mathbf{C} \leftarrow \mathbf{C} \text{Exp}m(-\mathbf{m}_C) \approx \mathbf{C}(\mathbf{I}_d - \mathbf{m}_C)$ 2: $\mathbf{M}_\mu \leftarrow \alpha_2 \mathbf{M}_\mu + \mathbf{C} \mathbf{C}^T \text{vec}^{-1}(\nabla_{\boldsymbol{\mu}} \ell(\boldsymbol{\mu})) \mathbf{K} \mathbf{K}^T$ 3: $\boldsymbol{\mu} \leftarrow \boldsymbol{\mu} - \beta_2 (\text{vec}(\mathbf{M}_\mu) + \gamma \nabla_{\boldsymbol{\mu}}(\boldsymbol{\mu}))$	1: At Frequency $T$ , update $(\mathbf{K} \mathbf{K}^T)^{-1}, (\mathbf{C} \mathbf{C}^T)^{-1}, \mathbf{K} \mathbf{K}^T, \mathbf{C} \mathbf{C}^T$ Obtain $\boldsymbol{\mu}_{AA} \otimes \boldsymbol{\mu}_{GG}$ to approximate $\nabla_{\boldsymbol{\mu}}^2 \ell(\boldsymbol{\mu})$ $(\mathbf{K} \mathbf{K}^T)^{-1} \leftarrow \theta (\mathbf{K} \mathbf{K}^T)^{-1} + (1 - \theta) \boldsymbol{\mu}_{AA}$ $(\mathbf{C} \mathbf{C}^T)^{-1} \leftarrow \theta (\mathbf{C} \mathbf{C}^T)^{-1} + (1 - \theta) \boldsymbol{\mu}_{GG}$ $\mathbf{K} \mathbf{K}^T \leftarrow ((\mathbf{K} \mathbf{K}^T)^{-1} + \lambda \mathbf{I}_p)^{-1}$ $\mathbf{C} \mathbf{C}^T \leftarrow ((\mathbf{C} \mathbf{C}^T)^{-1} + \lambda \mathbf{I}_d)^{-1}$ 2: $\mathbf{M}_\mu \leftarrow \alpha_2 \mathbf{M}_\mu + \mathbf{C} \mathbf{C}^T \text{vec}^{-1}(\nabla_{\boldsymbol{\mu}} \ell(\boldsymbol{\mu})) \mathbf{K} \mathbf{K}^T$ 3: $\boldsymbol{\mu} \leftarrow \boldsymbol{\mu} - \beta_2 (\text{vec}(\mathbf{M}_\mu) + \gamma \nabla_{\boldsymbol{\mu}}(\boldsymbol{\mu}))$

Figure 2. In our update, we denote  $\mathbf{H}_K := \mathbf{K}^T \boldsymbol{\mu}_{AA} \mathbf{K}$ ,  $\mathbf{H}_C := \mathbf{C}^T \boldsymbol{\mu}_{GG} \mathbf{C}$ ,  $k^2 := \lambda \text{Tr}(\mathbf{K}^T \mathbf{K})$ , and  $c^2 := \lambda \text{Tr}(\mathbf{C}^T \mathbf{C})$ , where  $\text{vec}^{-1}(\boldsymbol{\mu}) \in \mathbb{R}^{d \times p}$ ,  $\mathbf{C} \in \mathbb{R}^{d \times d}$ ,  $\mathbf{K} \in \mathbb{R}^{p \times p}$ . We use a linear truncation of the matrix exponential function. Our update does not require explicit matrix inverses. We can also pre-compute  $\mathbf{C} \mathbf{C}^T$  and  $\mathbf{K} \mathbf{K}^T$  when  $T > 1$ . In KFAC, a damping term  $\lambda \mathbf{I}$  is introduced to handle the non-singularity of  $(\mathbf{K} \mathbf{K}^T)^{-1}$  and  $(\mathbf{C} \mathbf{C}^T)^{-1}$ . We introduce a similar damping term in  $k^2$  and  $c^2$  (see Appx. I for a derivation) to improve numerical stability. Our update and KFAC include momentum weight  $\alpha_2$  for layer-wise NN weights  $\boldsymbol{\mu}$  and (L2) weight decay  $\gamma$ . In our update, we also introduce momentum weight  $\alpha_1$  in the SPD preconditioner.

by changing the normal coordinate to  $\mathbf{S}^{-1} = \boldsymbol{\tau} = \mathbf{A} \mathbf{A}^T$  where  $\mathbf{A} = \mathbf{A}^{(\text{cur})} \text{Exp}m(\frac{1}{2} \boldsymbol{\eta})$ .

To approximate the Hessian  $\nabla_{\boldsymbol{\mu}}^2 \ell(\boldsymbol{\mu})$  in deep learning as required in  $\mathbf{g}_\Sigma$ , we consider the KFAC approximation (Martens & Grosse, 2015). For simplicity, consider the loss function  $\ell(\boldsymbol{\mu})$  defined by one hidden layer of NN, where  $\text{vec}^{-1}(\boldsymbol{\mu}) \in \mathbb{R}^{d \times p}$  is a learnable weight matrix,  $\text{vec}(\cdot)$  is the vectorization function. In KFAC (summarized in Fig. 2), the Hessian at each layer of a neural network (NN) is approximated by a Kronecker-product structure between two dense symmetric positive semi-definite matrices as  $\nabla_{\boldsymbol{\mu}}^2 \ell(\boldsymbol{\mu}) \approx \boldsymbol{\mu}_{AA} \otimes \boldsymbol{\mu}_{GG}$ , where matrices  $\boldsymbol{\mu}_{AA} \in \mathbb{R}^{p \times p}$  and  $\boldsymbol{\mu}_{GG} \in \mathbb{R}^{d \times d}$  are computed as suggested by the authors and  $\otimes$  denotes the Kronecker product.

Motivated by KFAC, we consider a Kronecker-product structured SPD submanifold,

$$\mathcal{M} = \left\{ \boldsymbol{\tau} = \mathbf{U} \otimes \mathbf{W} \in \mathbb{R}^{pd \times pd} \mid \boldsymbol{\tau} \succ 0 \right\},$$

where matrices  $\mathbf{U} \in \mathbb{R}^{p \times p}$  and  $\mathbf{W} \in \mathbb{R}^{d \times d}$  are both SPD.

We can reexpress this submanifold as:

$$\mathcal{M} = \left\{ \boldsymbol{\tau} = \mathbf{A} \mathbf{A}^T \mid \mathbf{A} := \mathbf{K} \otimes \mathbf{C} \right\}, \quad (18)$$

where  $\mathbf{U} = \mathbf{K} \mathbf{K}^T$ ,  $\mathbf{W} = \mathbf{C} \mathbf{C}^T$ ,  $\mathbf{K} \in \mathbb{R}^{p \times p}$ ,  $\mathbf{C} \in \mathbb{R}^{d \times d}$ .  $\mathbf{K}$  and  $\mathbf{C}$  are (sub)groups of  $\text{GL}^{p \times p}$  and  $\text{GL}^{d \times d}$ , respectively.

By exploiting the Kronecker structure in  $\mathbf{A} = \mathbf{K} \otimes \mathbf{C}$ , we can simplify the update of  $\boldsymbol{\mu}$  in (17) as:

$$\boldsymbol{\mu} \leftarrow \boldsymbol{\mu} - \beta \mathbf{C} \mathbf{C}^T \text{vec}^{-1}(\mathbf{g}_\mu) \mathbf{K} \mathbf{K}^T. \quad (19)$$

Now, we describe how to update  $\mathbf{A} = \mathbf{K} \otimes \mathbf{C}$  by using the structure of the SPD submanifold  $\boldsymbol{\tau} = \mathbf{A} \mathbf{A}^T$ . Unfortunately, the affine invariant metric defined in Eq. (3) is singular. To enable the usage of this submanifold, we consider a block-diagonal approximation to update blocks  $\mathbf{K}$  and  $\mathbf{C}$ . Given each block, we construct a normal coordinate to trivialize the metric with respect to the block while

keeping the other block frozen. Such an approximation of the metric leads to a block-diagonal approximated metric. For blocks  $\mathbf{K}$  and  $\mathbf{C}$ , we consider the following blockwise normal coordinates  $\boldsymbol{\eta}_K$  and  $\boldsymbol{\eta}_C$ , respectively:

$$\begin{aligned} \mathbf{A} &= \left( \mathbf{K}^{(\text{cur})} \text{Exp}m \left( \frac{1}{2\sqrt{d}} \boldsymbol{\eta}_K \right) \right) \otimes \mathbf{C}^{(\text{cur})}, \\ \mathbf{A} &= \mathbf{K}^{(\text{cur})} \otimes \left( \mathbf{C}^{(\text{cur})} \text{Exp}m \left( \frac{1}{2\sqrt{p}} \boldsymbol{\eta}_C \right) \right), \end{aligned} \quad (20)$$

where both  $\boldsymbol{\eta}_K \in \mathbb{R}^{p \times p}$  and  $\boldsymbol{\eta}_C \in \mathbb{R}^{d \times d}$  are symmetric matrices and  $\mathbf{A}^{(\text{cur})} = \mathbf{K}^{(\text{cur})} \otimes \mathbf{C}^{(\text{cur})}$ . The scalars highlighted in red are needed to trivialize the (block-diagonal) metric.

Using these blockwise normal coordinates, our update is summarized in Fig. 2 (see Appx. I for a derivation), where similar to KFAC, we further introduce momentum weight  $\alpha_2$  for  $\boldsymbol{\mu}$ , weight decay  $\gamma$ , and damping weight  $\lambda$ . In practice, we truncate the matrix exponential function: the quadratic truncation  $\text{Exp}m(\mathbf{N}) \approx \mathbf{I} + \mathbf{N} + \frac{1}{2} \mathbf{N}^2$  ensures the non-singularity of  $\mathbf{K}$  and  $\mathbf{C}$ . In our experiments, we observed that the linear truncation  $\text{Exp}m(\mathbf{N}) \approx \mathbf{I} + \mathbf{N}$  also works well for deep learning problems.

We can also develop sparse Kronecker factor updates while KFAC does not admit a sparse update. Our approach allows us to include more sparse structures by considering  $\mathbf{K}$  and  $\mathbf{C}$  to have sparse group structures in Eq. (18).

## 5. Numerical Results

### 5.1. Results on Synthetic Examples

To validate our proposed updates, we consider a full SPD manifold and a SPD submanifold.

In the first example, we consider manifold optimization on full SPD matrices  $\mathcal{S}_{++}^{d \times d}$  with  $d = 100$ , where the Riemannian maps admit a closed-form expression (shown in Table 1). We evaluate our method on an example of the

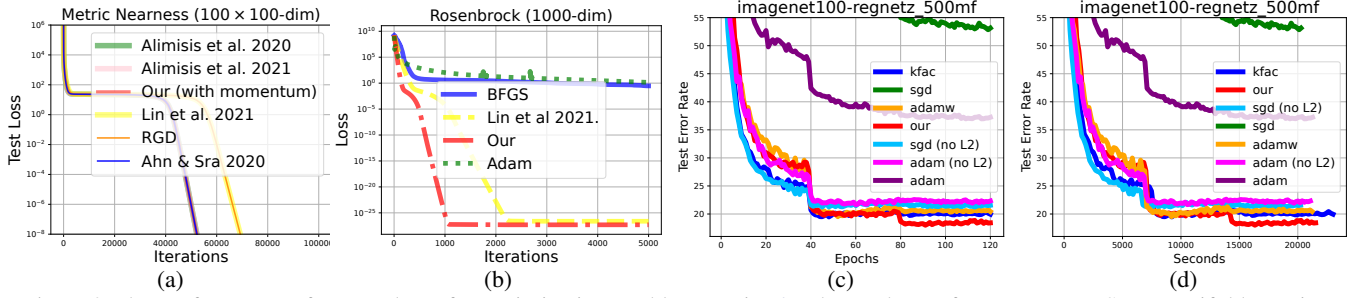


Figure 3. The performance of our updates for optimization problems. Fig. 3a shows the performance on a SPD manifold matrix optimization. Our update using approximations of the Riemannian maps achieves a similar performance as existing Riemannian methods using the exact Riemannian maps. Fig. 3b shows the performance using a structured SPD preconditioner to optimize a 1000-dimensional function, where our update and structured NGD make use of Hessian information without computing the full Hessian. Our update with momentum converges faster than structured NGD, BFGS and Adam. Fig. 3c-3d shows the performance for optimization in NN models. Our updates achieve lower test error rates than the other methods.

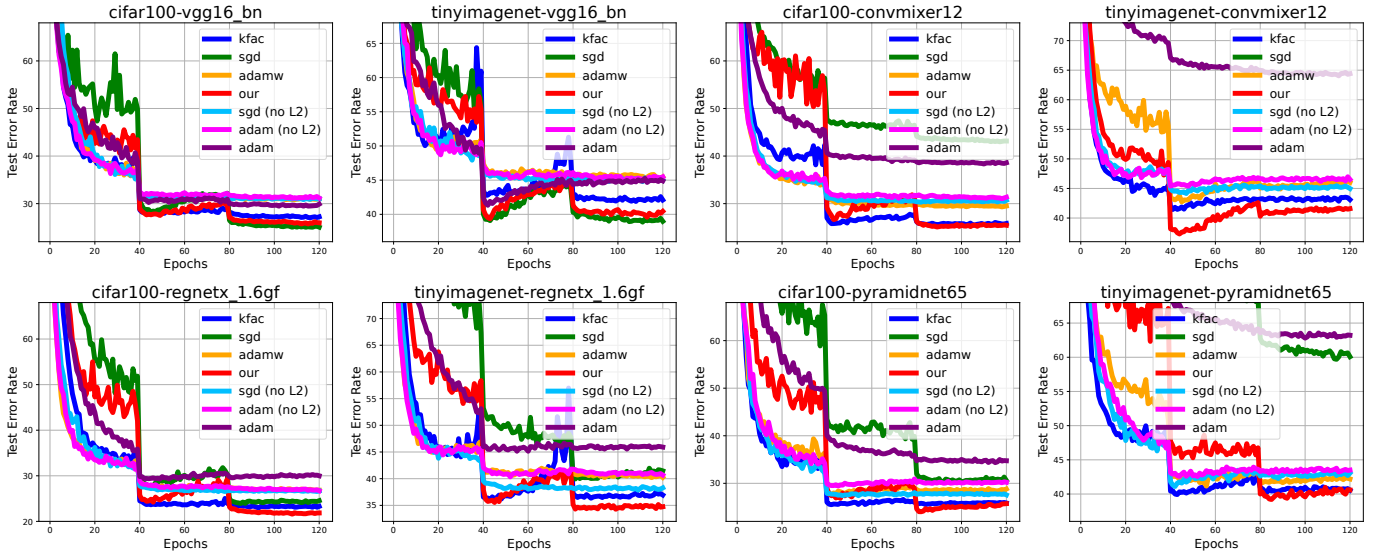


Figure 4. Fig. 4 and 5 show the performance for optimization in NN models. SGD performs best in the classical model and fairly in the modern models. Our updates achieve competitive test error rates compared to baselines and perform better than KFAC in many cases.

metric nearness problem considered in Lin et al. (2021a). We consider structured NGD (Lin et al., 2021a), RGD, and existing Riemannian momentum methods such as the ones presented by Ahn & Sra (2020), Alimisis et al. (2020; 2021) as baselines. All methods are trained using mini-batches with a mini-batch size of 250. From Fig. 3a, we can see that our method performs as well as the Riemannian methods with the exact Riemannian maps in the global coordinate.

In the second example, we minimize a 1000-dim Rosenbrock function. We consider the inverse of the preconditioner  $\tau = \mathbf{S}^{-1}$  in Eq. (16) as a SPD submanifold. We include momentum in  $\tau$  and  $\mu$ . We compare our update with structured NGD, where both methods use the Heisenberg structure suggested by Lin et al. (2021a) to construct a submanifold. Both methods make use of Hessian information without computing the full Hessian. We consider other baselines: BFGS and Adam. We tune the step-size for all

methods. From Fig. 3b, we can see that adding momentum in the preconditioner could be useful for optimization.

## 5.2. Results in Deep Learning

To demonstrate our method as a practical Riemannian method in high-dimensional cases, we consider image classification tasks with NN architectures ranging from classical to modern models: VGG-16 (Simonyan & Zisserman, 2014) with the batch normalization, PyramidNet-65 (Han et al., 2017), RegNetX-1.6GF (Radosavovic et al., 2020), RegNetZ-500MF (Dollár et al., 2021), RepVGG-B1G4 (Ding et al., 2021), and ConvMixer-12 (Trockman & Kolter, 2022). We use the KFAC approximation for convolution layers (Grosse & Martens, 2016). Table 6 in Appx. A summarizes the number of learnable parameters. We consider three complex datasets “CIFAR-100”, “TinyImageNet-

## Simplifying Momentum-based Riemannian Submanifold Optimization

Dataset	Method	VGG-16	PyramidNet-65	ConvMixer-12	RegNetX-1.6GF
CIFAR-100	SGD (No L2)	<b>25.13</b> (31.01)	30.87 (27.71)	43.13 (30.54)	24.34 (26.67)
	Adam (No L2)	29.60 (31.33)	34.67 (30.20)	38.56 (31.24)	30.093 (26.93)
	AdamW	31.04	28.59	29.46	26.95
	KFAC	27.16	25.92	25.81	23.25
	Ours	25.92	<b>25.45</b>	<b>25.44</b>	<b>21.78</b>
TinyImageNet-200	SGD (No L2)	<b>39.12</b> (45.05)	60.36 (42.94)	74.90 (45.26)	41.33 (38.21)
	Adam (No L2)	44.93 (45.34)	63.16 (43.48)	64.34 (46.61)	45.98 (40.89)
	AdamW	45.49	42.27	45.96	40.41
	KFAC	42.20	40.73	43.25	37.01
	Ours	40.03	<b>40.42</b>	<b>41.52</b>	<b>34.80</b>

Table 3. The performance of the methods in terms of the test error rate. The results are obtained by averaging over the last 10 iterations.

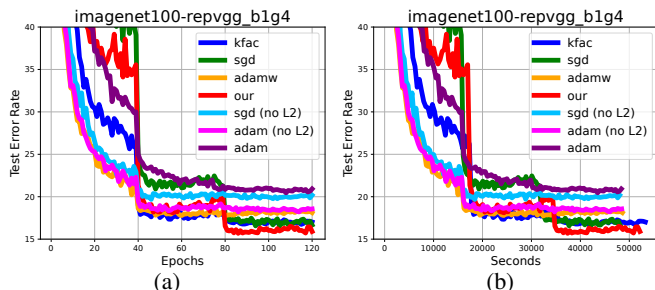


Figure 5. Fig. 5 shows more results on ImageNet-100.

200”<sup>1</sup>, and “ImageNet-100”<sup>2</sup>. The hyper-parameter configuration of our update and KFAC can be found in Table 5 in Appx. A. We also consider built-in baselines in PyTorch such as SGD with momentum, Adam, and AdamW. By default, a L2 weight decay is included in all methods. We also consider a version of SGD and Adam denoted by “No L2”, where no weight decay is added. We train all models from scratch for 120 epochs with mini-batch size 128. For all methods, we tune the initial step-size and then divide the step-size by 10 every 40 epochs, as suggested by Wilson et al. (2017). Our method can take a larger stepsize than KFAC for all the NN models. Our method has similar running times as KFAC, as shown in Fig. 3d and 5b in the main text, and Fig. 6 in Appx. A. We report the test error rate (i.e., error rate = 100 – accuracy percentage) for all methods in Table 3 and 4. From Fig. 3c, 3d 4, and 5, we can see that our method performs better than KFAC and achieves competitive performances among other baselines.

Our Pytorch implementation will soon be made available<sup>3</sup>.

## 6. Conclusion

We propose generalized normal coordinates to simplify existing Riemannian optimization methods, which results in efficient NGD with momentum updates. Our approach expands the scope of structured NGD to SPD submanifolds

<sup>1</sup>[github.com/tjmoon0104/pytorch-tiny-imagenet](https://github.com/tjmoon0104/pytorch-tiny-imagenet)

<sup>2</sup>[kaggle.com/datasets/ambityga/imagenet100](https://kaggle.com/datasets/ambityga/imagenet100)

<sup>3</sup>[github.com/yorkerlin/StructuredNGD-DL](https://github.com/yorkerlin/StructuredNGD-DL)

Dataset	Method	RegNetZ-500MF	RepVGG-B1G4
ImagetNet-100	SGD (No L2)	53.28 (21.45)	17.03 (20.06)
	Adam (No L2)	37.13 (22.18)	20.78 (18.46)
	AdamW	20.58	18.23
	KFAC	20.07	16.97
	Ours	<b>18.58</b>	<b>16.14</b>

Table 4. The performance (test error rate) of the methods obtained by averaging over the last 10 iterations.

arising in machine learning applications and enables the usage of structured NGD beyond Bayesian and Gaussian settings from a deterministic matrix manifold optimization perspective. We further develop efficient structured optimizers for deep learning. An interesting application is to design customized optimizers for a given NN architecture. Overall, our work provides a new way to design practical manifold optimization methods.

## References

- Absil, P.-A., Mahony, R., and Sepulchre, R. *Optimization algorithms on matrix manifolds*. Princeton University Press, 2009.
- Ahn, K. and Sra, S. From Nesterov’s estimate sequence to Riemannian acceleration. In *Conference on Learning Theory*, pp. 84–118. PMLR, 2020.
- Alimisis, F., Orvieto, A., Bécigneul, G., and Lucchi, A. A continuous-time perspective for modeling acceleration in Riemannian optimization. In *International Conference on Artificial Intelligence and Statistics*, pp. 1297–1307. PMLR, 2020.
- Alimisis, F., Orvieto, A., Becigneul, G., and Lucchi, A. Momentum improves optimization on riemannian manifolds. In *International Conference on Artificial Intelligence and Statistics*, pp. 1351–1359. PMLR, 2021.
- Bonnabel, S. Stochastic gradient descent on Riemannian

- manifolds. *IEEE Transactions on Automatic Control*, 58(9):2217–2229, 2013.
- Calvo, M. and Oller, J. M. A distance between multivariate normal distributions based in an embedding into the Siegel group. *Journal of multivariate analysis*, 35(2): 223–242, 1990.
- Cherian, A. and Sra, S. Riemannian dictionary learning and sparse coding for positive definite matrices. *IEEE transactions on neural networks and learning systems*, 28(12):2859–2871, 2016.
- Ding, X., Zhang, X., Ma, N., Han, J., Ding, G., and Sun, J. Repvgg: Making vgg-style convnets great again. In *Proceedings of the IEEE/CVF conference on computer vision and pattern recognition*, pp. 13733–13742, 2021.
- Dollár, P., Singh, M., and Girshick, R. Fast and accurate model scaling. In *Proceedings of the IEEE/CVF Conference on Computer Vision and Pattern Recognition*, pp. 924–932, 2021.
- Girolami, M. and Calderhead, B. Riemann manifold langevin and hamiltonian monte carlo methods. *Journal of the Royal Statistical Society: Series B (Statistical Methodology)*, 73(2):123–214, 2011.
- Godaz, R., Ghojogh, B., Hosseini, R., Monsefi, R., Karray, F., and Crowley, M. Vector transport free riemannian lbfgs for optimization on symmetric positive definite matrix manifolds. In *Asian Conference on Machine Learning*, pp. 1–16. PMLR, 2021.
- Grosse, R. and Martens, J. A kronecker-factored approximate fisher matrix for convolution layers. In *International Conference on Machine Learning*, pp. 573–582. PMLR, 2016.
- Guillaumin, M., Verbeek, J., and Schmid, C. Is that you? metric learning approaches for face identification. In *2009 IEEE 12th international conference on computer vision*, pp. 498–505. IEEE, 2009.
- Han, D., Kim, J., and Kim, J. Deep pyramidal residual networks. In *Proceedings of the IEEE conference on computer vision and pattern recognition*, pp. 5927–5935, 2017.
- Hosseini, R. and Sra, S. Matrix manifold optimization for Gaussian mixtures. In *Advances in Neural Information Processing Systems*, pp. 910–918, 2015.
- Jeuris, B., Vandebril, R., and Vandereycken, B. A survey and comparison of contemporary algorithms for computing the matrix geometric mean. *Electronic Transactions on Numerical Analysis*, 39(ARTICLE):379–402, 2012.
- Khan, M. and Lin, W. Conjugate-computation variational inference: Converting variational inference in non-conjugate models to inferences in conjugate models. In *Artificial Intelligence and Statistics*, pp. 878–887, 2017.
- Lezcano, C.-M. Trivializations for gradient-based optimization on manifolds. *Advances in Neural Information Processing Systems*, 32:9157–9168, 2019.
- Lezcano, C.-M. Adaptive and momentum methods on manifolds through trivializations. *arXiv preprint arXiv:2010.04617*, 2020.
- Lin, W., Nielsen, F., Emtiyaz, K. M., and Schmidt, M. Tractable structured natural-gradient descent using local parameterizations. In *International Conference on Machine Learning*, pp. 6680–6691. PMLR, 2021a.
- Lin, W., Nielsen, F., Khan, M. E., and Schmidt, M. Structured second-order methods via natural gradient descent. *arXiv preprint arXiv:2107.10884*, 2021b.
- Makam, V., Reichenbach, P., and Seigal, A. Symmetries in directed gaussian graphical models. *arXiv preprint arXiv:2108.10058*, 2021.
- Martens, J. and Grosse, R. Optimizing neural networks with Kronecker-factored approximate curvature. In *International Conference on Machine Learning*, pp. 2408–2417, 2015.
- Minh, H. Q. and Murino, V. Covariances in computer vision and machine learning. *Synthesis Lectures on Computer Vision*, 7(4):1–170, 2017.
- Radosavovic, I., Kosaraju, R. P., Girshick, R., He, K., and Dollár, P. Designing network design spaces. In *Proceedings of the IEEE/CVF conference on computer vision and pattern recognition*, pp. 10428–10436, 2020.
- Simonyan, K. and Zisserman, A. Very deep convolutional networks for large-scale image recognition. *arXiv preprint arXiv:1409.1556*, 2014.
- Slawski, M., Li, P., and Hein, M. Regularization-free estimation in trace regression with symmetric positive semidefinite matrices. *Advances in Neural Information Processing Systems*, 28, 2015.
- Trockman, A. and Kolter, J. Z. Patches are all you need? *arXiv preprint arXiv:2201.09792*, 2022.
- Wang, C., Sun, D., and Toh, K.-C. Solving log-determinant optimization problems by a newton-cg primal proximal point algorithm. *SIAM Journal on Optimization*, 20(6): 2994–3013, 2010.

Wilson, A. C., Roelofs, R., Stern, M., Srebro, N., and Recht, B. The marginal value of adaptive gradient methods in machine learning. *Advances in neural information processing systems*, 30, 2017.

# Appendices

Outline of the Appendix:

- Appendix A contains more numerical results.
- Appendix B summarizes the normal coordinates used in this work.
- The rest of the appendix contains proofs of the claims and derivations for examples considered in the main text.

## A. Additional Results

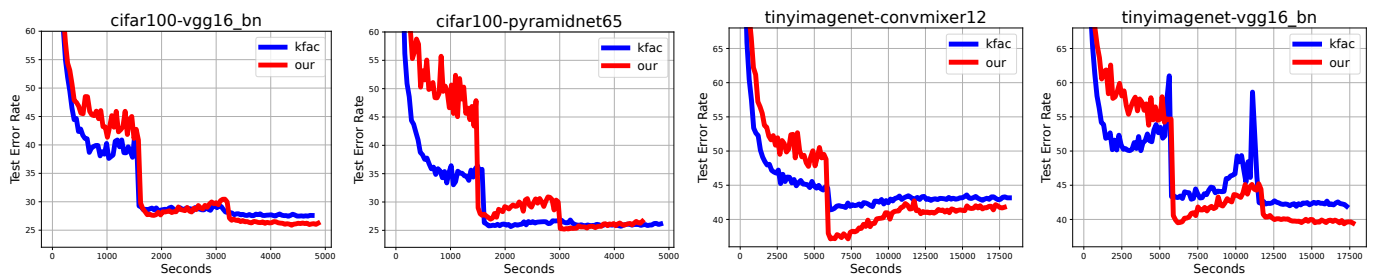


Figure 6. Additional results of our method and KFAC using a new random seed. We use these two methods to train NN models in 120 epochs. We report the performance of the methods in terms of running time.

Hyperparameter	Meanings	Our Method in Fig. 2	KFAC
$\beta_2$	Standard step-size	Tuned	Tuned
$\alpha_2$	Standard momentum weight	0.9	0.9
$\gamma$	(L2) weight decay	0.01	0.01
$\lambda$	Damping weight	0.01; 0.005; 0.0005	0.01; 0.005; 0.0005
$T$	Update frequency	10; 25; 60	10; 25; 60
$\theta$	Moving average in KFAC	NA	0.95
$\beta_1$	Stepsize to update our preconditioner	0.01	NA
$\alpha_1$	Momentum weight to update our preconditioner	0.5	NA

Table 5. Hyperparameter configuration in our update and KFAC. We first choose the damping weight  $\lambda$  according to the performance of KFAC and use the same value in our update. For the both methods, we set  $\lambda = 0.01, 0.0005, 0.005$  in VGG16, RepVGG-B1G4, and other models, respectively. To reduce the iteration cost of the both methods, we update the preconditioner at every  $T = 60, 25, 10$  iterations for RepVGG-B1G4, RegNetZ-500MF, and other models, respectively. The value of  $\theta$  is chosen as suggested at <https://github.com/alecwangcq/KFAC-Pytorch>. Since we do not use pre-training, we consider the first 500 iterations as a warm-up period to update our preconditioner by using a smaller stepsize  $\beta_1$ . For the first 100 iterations, we set  $\beta_1 = 0.0002$ , then increase it to 0.002 at the following 400 iterations, and finally fix it to 0.01 afterwards.

## Simplifying Momentum-based Riemannian Submanifold Optimization

Dataset	VGG-16-BN	PyramidNet-65	ConvMixer-12	RegNetX-1.6GF
CIFAR-100	14,774,436	707,428	911,204	8,368,436
TinyImageNet-200	14,825,736	733,128	936,904	8,459,736

Dataset	RegNetZ-500MF	RepVGG-B1G4
ImageNet-100	6,200,242	38,121,956

Table 6. Number of Learnable NN Parameters

Dataset	Input Dimension	Number of Classes	Number of Training Points	Number of Test Points
CIFAR-100	$32 \times 32$	100	50,000	10,000
TinyImageNet-200	$64 \times 64$	200	100,000	5,000
ImageNet-100	$224 \times 224$	100	130,000	5,000

Table 7. Statistics of the Datasets

## B. Summary of Generalized Normal Coordinates

SPD (sub)manifold $\mathcal{M}$	Name	Our normal coordinate
$\{\boldsymbol{\tau} \in \mathbb{R}^{k \times k} \mid \boldsymbol{\tau} \in \mathcal{S}_{++}^{k \times k}\}$ with affine invariant metric $\mathbf{F}$	Full manifold	See Eq. (11)
$\left\{ \boldsymbol{\tau} = \begin{bmatrix} \mathbf{V} & \boldsymbol{\mu} \\ \boldsymbol{\mu}^T & 1 \end{bmatrix} \in \mathbb{R}^{k \times k} \mid \boldsymbol{\tau} \in \mathcal{S}_{++}^{k \times k} \right\}$ with affine invariant metric $\mathbf{F}$	submanifold induced by Siegel embedding	See Eq. (12),(13)
$\left\{ \boldsymbol{\tau} = \mathbf{U} \otimes \mathbf{W} \in \mathbb{R}^{pd \times pd} \mid \mathbf{U} \in \mathcal{S}_{++}^{p \times p}, \mathbf{W} \in \mathcal{S}_{++}^{d \times d} \right\}$ with an approximated affine invariant metric $\mathbf{F}$	Kronecker-product submanifold	See Eq. (20)

Table 8. Summary of our normal coordinates, where  $\mathcal{S}_{++}$  denotes the set of SPD matrices

## C. Background

In this section, we will assume  $\boldsymbol{\tau}$  is a (learnable) vector to simplify notations. For a SPD matrix  $\mathbf{M} \in \mathcal{S}_{++}^{k \times k}$ , we could consider  $\boldsymbol{\tau} = \text{vech}(\mathbf{M})$ , where  $\text{vech}(\mathbf{M})$  returns a  $\frac{k(k+1)}{2}$ -dimensional array obtained by vectorizing only the lower triangular part of  $\mathbf{M}$ , which is known as the half-vectorization function.

### C.1. Fisher-Rao Metric

Under parametrization  $\boldsymbol{\tau}$ , the Fisher-Rao Metric is defined as

$$\mathbf{F}(\boldsymbol{\tau}^{(\text{cur})}) := -E_{q(\mathbf{z}|\boldsymbol{\tau})}[\nabla_{\boldsymbol{\tau}}^2 \log q(\mathbf{z}|\boldsymbol{\tau})] \Big|_{\boldsymbol{\tau}=\boldsymbol{\tau}^{(\text{cur})}}, \quad (21)$$

where  $q(\mathbf{z}|\boldsymbol{\tau})$  is a probabilistic distribution parameterized by  $\boldsymbol{\tau}$ , such as a Gaussian distribution with zero mean and covariance  $\boldsymbol{\tau}$ .

### C.2. Christoffel Symbols

Given a Riemannian metric  $\mathbf{F}$ , the Christoffel symbols of the first kind are defined as

$$\Gamma_{d,ab}(\boldsymbol{\tau}_1) := \frac{1}{2}[\partial_a F_{bd}(\boldsymbol{\tau}) + \partial_b F_{ad}(\boldsymbol{\tau}) - \partial_d F_{ab}(\boldsymbol{\tau})] \Big|_{\boldsymbol{\tau}=\boldsymbol{\tau}_1}, \quad (22)$$

where  $F_{bd}(\boldsymbol{\tau})$  denotes the  $(b, d)$  entry of the metric  $\mathbf{F}_{\boldsymbol{\tau}}$  and  $\partial_b$  denotes the partial derivative w.r.t. the  $b$ -th entry of  $\boldsymbol{\tau}$ .

The Christoffel symbols of the second kind are defined as  $\Gamma_{ab}^c(\boldsymbol{\tau}) := \sum_d F^{cd}(\boldsymbol{\tau})\Gamma_{d,ab}(\boldsymbol{\tau})$  where  $F^{cd}(\boldsymbol{\tau})$  denotes the (c,d) entry of the inverse  $\mathbf{F}^{-1}$  of the metric. Observe that the Christoffel symbols of the second kind involve computing all partial derivatives of the metric  $\mathbf{F}$  and the inverse of the metric.

### C.3. Riemannian Exponential Map

The Riemannian exponential map is defined via a geodesic, which generalizes the notion of a straight line to a manifold. The geodesic  $\mathbf{r}(t)$  satisfies the following second-order nonlinear system of ODEs with initial values  $\mathbf{r}(0) = \mathbf{x}$  and  $\dot{\mathbf{r}}(0) = \boldsymbol{\nu}$ , where  $\mathbf{x}$  denotes a point on the manifold and  $\boldsymbol{\nu}$  is a Riemannian gradient,

$$\text{geodesic ODE: } \ddot{r}^c(t) + \sum_{a,b} \Gamma_{ab}^c(\mathbf{r}(t))\dot{r}^a(t)\dot{r}^b(t) = 0, \quad (23)$$

where  $r^c(t)$  denotes the  $c$ -th entry and  $\Gamma_{ab}^c$  is the Christoffel symbol of the second kind.

The Riemannian exponential map is defined as

$$\text{RExp}(\mathbf{x}, \boldsymbol{\nu}) := \mathbf{r}(1), \quad (24)$$

where  $\mathbf{x}$  denotes an initial point and  $\boldsymbol{\nu}$  is an initial Riemannian gradient so that  $\mathbf{r}(0) = \mathbf{x}$  and  $\dot{\mathbf{r}}(0) = \boldsymbol{\nu}$ .

### C.4. Riemannian (Parallel) Transport Map

In a curved space, the transport map along a given curve generalizes the notion of parallel transport. In Riemannian optimization, we consider the transport map along a geodesic curve. Given a geodesic curve  $\mathbf{r}(t)$ , denote by  $\mathbf{v}(t)$  a smooth Riemannian gradient field that satisfies the following first-order linear system of ODEs with initial value  $\mathbf{v}(0) = \boldsymbol{\nu}$ ,

$$\text{transport ODE: } \dot{v}^c(t) + \sum_{a,b} \Gamma_{ab}^c(\mathbf{r}(t))v^a(t)\dot{r}^b(t) = 0. \quad (25)$$

This transport map  $\hat{T}_{\boldsymbol{\tau}^{(\text{old})} \rightarrow \boldsymbol{\tau}^{(\text{old})}}(\boldsymbol{\nu})$  transports the Riemannian gradient  $\boldsymbol{\nu}$  at  $\boldsymbol{\tau}^{(\text{old})}$  to  $\boldsymbol{\tau}^{(\text{new})}$  as follows,

$$\hat{T}_{\boldsymbol{\tau}^{(\text{cur})} \rightarrow \boldsymbol{\tau}^{(\text{new})}}(\boldsymbol{\nu}) := \mathbf{v}(1), \quad (26)$$

where  $\mathbf{r}(0) = \boldsymbol{\tau}^{(\text{cur})}$ ,  $\mathbf{r}(1) = \boldsymbol{\tau}^{(\text{new})}$ , and  $\mathbf{v}(0) = \boldsymbol{\nu}$ . It can be computationally challenging to solve this linear ODE due to the Christoffel symbols.

### C.5. Euclidean (Parallel) Transport Map

Given a geodesic curve  $\mathbf{r}(t)$ , denote by  $\boldsymbol{\omega}(t)$  a smooth Euclidean gradient field on manifold  $\mathcal{M}$  that satisfies the following first-order linear system of ODEs with initial value  $\boldsymbol{\omega}(0) = \mathbf{m}$ ,

$$\text{transport ODE: } \dot{\omega}_c(t) - \sum_{a,b} \Gamma_{cb}^a(\mathbf{r}(t))\omega_a(t)\dot{r}^b(t) = 0. \quad (27)$$

The transport map transports the Euclidean gradient  $\mathbf{g}$  at  $\boldsymbol{\tau}^{(\text{cur})}$  to  $\boldsymbol{\tau}^{(\text{new})}$  as shown below,

$$T_{\boldsymbol{\tau}^{(\text{cur})} \rightarrow \boldsymbol{\tau}^{(\text{new})}}(\mathbf{g}) := \boldsymbol{\omega}(1), \quad (28)$$

where  $\mathbf{r}(0) = \boldsymbol{\tau}^{(\text{cur})}$ ,  $\mathbf{r}(1) = \boldsymbol{\tau}^{(\text{new})}$ , and  $\boldsymbol{\omega}(0) = \mathbf{g}$ .

These two transport maps are related as follows,

$$\hat{T}_{\boldsymbol{\tau}^{(\text{cur})} \rightarrow \boldsymbol{\tau}^{(\text{new})}}(\mathbf{F}_{\boldsymbol{\tau}^{(\text{cur})}}^{-1}(\boldsymbol{\tau}^{(\text{cur})})\mathbf{g}) = \mathbf{F}_{\boldsymbol{\tau}^{(\text{new})}}^{-1}(\boldsymbol{\tau}^{(\text{new})})T_{\boldsymbol{\tau}^{(\text{cur})} \rightarrow \boldsymbol{\tau}^{(\text{new})}}(\mathbf{g}), \quad (29)$$

where  $\mathbf{g}$  is a Euclidean gradient evaluated at  $\boldsymbol{\tau}^{(\text{cur})}$ .

### C.6. Update 2 is Equivalent to Alimisis et al. (2020)

Alimisis et al. (2020) propose the following Riemannian momentum update:

$$\begin{aligned}\boldsymbol{\nu}^{(\text{cur})} &\leftarrow \beta \mathbf{z}^{(\text{cur})} + \alpha \mathbf{F}_{\tau}^{-1}(\boldsymbol{\tau}^{(\text{cur})}) \mathbf{g}(\boldsymbol{\tau}^{(\text{cur})}), \\ \boldsymbol{\tau}^{(\text{new})} &\leftarrow \text{REXP}(\boldsymbol{\tau}^{(\text{cur})}, -\boldsymbol{\nu}^{(\text{cur})}), \\ \mathbf{z}^{(\text{new})} &\leftarrow \hat{T}_{\boldsymbol{\tau}^{(\text{cur})} \rightarrow \boldsymbol{\tau}^{(\text{new})}}(\boldsymbol{\nu}^{(\text{cur})}),\end{aligned}\tag{30}$$

where  $\boldsymbol{\nu}$  is a Riemannian gradient, and  $\hat{T}_{\boldsymbol{\tau}^{(\text{cur})} \rightarrow \boldsymbol{\tau}^{(\text{new})}}$  is the Riemannian (parallel) transport map.

Due to Eq. (29), updates (30) and (2) are equivalent since  $\mathbf{m}^{(\text{cur})} = \mathbf{F}(\boldsymbol{\tau}^{(\text{cur})})\boldsymbol{\nu}^{(\text{cur})}$  and  $\mathbf{w}^{(\text{new})} = \mathbf{F}(\boldsymbol{\tau}^{(\text{new})})\mathbf{z}^{(\text{new})}$ , where  $\mathbf{m}^{(\text{cur})}$  and  $\mathbf{w}^{(\text{new})}$  are defined in Eq. (2).

## D. Simplification of the vector-Jacobian Product

The vector-Jacobian product in (10) could, in general, be computed by automatic differentiation. We give two cases for SPD (sub)manifolds where the product can be explicitly simplified.

For notation simplicity, we denote  $\mathbf{m} = \mathbf{m}^{(\eta_0)}$  and  $\mathbf{w} = \mathbf{w}^{(\eta_1)}$ . Thus  $\mathbf{w} = \mathbf{m}$  when we use the approximation in Eq. (9).

### D.1. Symmetric Cases

Suppose that  $\boldsymbol{\eta}$  is symmetric, in which case  $\mathbf{m}$  is also symmetric due to update (8). We further denote  $\mathbf{A}_0 = \mathbf{A}^{(\text{cur})}$  and  $\mathbf{A}_1 = \mathbf{A}^{(\text{new})}$ , where  $\mathbf{A}_1 = \mathbf{A}_0 \text{Exp}(\mathbf{m}) = \mathbf{A}_0 \text{Exp}(\mathbf{m})$ .

Recall that  $\boldsymbol{\tau} = \mathbf{A}_0 \text{Exp}(\boldsymbol{\eta}) \mathbf{A}_0^T = \mathbf{A}_1 \text{Exp}(\boldsymbol{\xi}) \mathbf{A}_1^T$ . Thus, we have

$$\text{Exp}(\boldsymbol{\eta}) = \text{Exp}(-\frac{1}{2}\mathbf{m}) \text{Exp}(\boldsymbol{\xi}) \text{Exp}^T(-\frac{1}{2}\mathbf{m}) = \text{Exp}(-\frac{1}{2}\mathbf{m}) \text{Exp}(\boldsymbol{\xi}) \text{Exp}(-\frac{1}{2}\mathbf{m}).$$

By the Baker-Campbell-Hausdorff formula, we have

$$\begin{aligned}\text{Exp}^{-1}(\text{Exp}(\mathbf{N})\text{Exp}(\mathbf{M})) &= \mathbf{N} + \mathbf{M} + \sum_i w_i (\mathbf{M}^{a_i} \mathbf{N} \mathbf{M}^{b_i} - \mathbf{M}^{c_i} \mathbf{N} \mathbf{M}^{d_i}) + O(\mathbf{N}^2), \\ \text{Exp}^{-1}(\text{Exp}(\mathbf{M})\text{Exp}(\mathbf{N})) &= \mathbf{N} + \mathbf{M} + \sum_i w_i (\mathbf{M}^{a_i} \mathbf{N} \mathbf{M}^{b_i} - \mathbf{M}^{c_i} \mathbf{N} \mathbf{M}^{d_i}) + O(\mathbf{N}^2),\end{aligned}$$

where  $a_i + b_i = c_i + d_i > 0$ , and  $a_i, b_i, c_i, d_i$  are non-negative integers and  $w_i$  is a coefficient.

Since we evaluate the Jacobian at  $\boldsymbol{\xi}_0 = \mathbf{0}$ , we can get rid of the higher order term  $O(\boldsymbol{\xi}^2)$ , which leads to the following simplification,

$$\boldsymbol{\eta} = \text{Exp}^{-1}(\text{Exp}(-\frac{1}{2}\mathbf{m})\text{Exp}(\boldsymbol{\xi})\text{Exp}(-\frac{1}{2}\mathbf{m})) = \boldsymbol{\xi} - \mathbf{m} + \sum_i w_i (\mathbf{m}^{a_i} \boldsymbol{\xi} \mathbf{m}^{b_i} - \mathbf{m}^{c_i} \boldsymbol{\xi} \mathbf{m}^{d_i}) + O(\boldsymbol{\xi}^2).$$

Recall that  $\mathbf{m} = \mathbf{w}$  is symmetric. The vector-Jacobian product can be simplified as

$$\begin{aligned}\mathbf{w}^T \mathbf{J}(\boldsymbol{\xi}_0) &= \mathbf{m}^T \left[ \frac{\partial \boldsymbol{\eta}}{\partial \boldsymbol{\xi}} \Big|_{\boldsymbol{\xi}=\boldsymbol{\xi}_0} \right] \\ &= \nabla_{\boldsymbol{\xi}} \text{Tr}(\mathbf{m}^T \boldsymbol{\eta}) \Big|_{\boldsymbol{\xi}=\boldsymbol{\xi}_0} \\ &= \nabla_{\boldsymbol{\xi}} \text{Tr}(\mathbf{m}^T [\boldsymbol{\xi} - \mathbf{m} + \sum_i w_i (\mathbf{m}^{a_i} \boldsymbol{\xi} \mathbf{m}^{b_i} - \mathbf{m}^{c_i} \boldsymbol{\xi} \mathbf{m}^{d_i}) + O(\boldsymbol{\xi}^2)]) \Big|_{\boldsymbol{\xi}=\boldsymbol{\xi}_0} \\ &= \nabla_{\boldsymbol{\xi}} \text{Tr}(\mathbf{m}^T [\boldsymbol{\xi} + \sum_i w_i (\mathbf{m}^{a_i} \boldsymbol{\xi} \mathbf{m}^{b_i} - \mathbf{m}^{c_i} \boldsymbol{\xi} \mathbf{m}^{d_i})]) \Big|_{\boldsymbol{\xi}=\boldsymbol{\xi}_0} \\ &= \nabla_{\boldsymbol{\xi}} \text{Tr}(\mathbf{m} [\boldsymbol{\xi} + \sum_i w_i (\mathbf{m}^{a_i} \boldsymbol{\xi} \mathbf{m}^{b_i} - \mathbf{m}^{c_i} \boldsymbol{\xi} \mathbf{m}^{d_i})]) \Big|_{\boldsymbol{\xi}=\boldsymbol{\xi}_0} \\ &= \nabla_{\boldsymbol{\xi}} \text{Tr}(\mathbf{m} \boldsymbol{\xi} + \sum_i w_i (\mathbf{m}^{a_i+b_i+1} \boldsymbol{\xi} - \mathbf{m}^{c_i+d_i+1} \boldsymbol{\xi})) \Big|_{\boldsymbol{\xi}=\boldsymbol{\xi}_0} \\ &= \nabla_{\boldsymbol{\xi}} \text{Tr}(\mathbf{m} \boldsymbol{\xi}) \Big|_{\boldsymbol{\xi}=\boldsymbol{\xi}_0} = \mathbf{m} = \mathbf{w}.\end{aligned}\tag{31}$$

## D.2. Triangular Cases

Without loss of generality, we assume  $\boldsymbol{\eta}$  is lower-triangular, in which case  $\mathbf{m}$  is also lower-triangular due to update (8). Similarly, we denote  $\mathbf{A}_0 = \mathbf{A}^{(\text{cur})}$  and  $\mathbf{A}_1 = \mathbf{A}^{(\text{new})}$ , where  $\mathbf{A}_1 = \mathbf{A}_0 \text{Exp}(\mathbf{D} \odot \mathbf{m}^{(\eta_0)}) = \mathbf{A}_0 \text{Exp}(\mathbf{D} \odot \mathbf{m})$ , where  $\mathbf{D} = \frac{1}{\sqrt{2}} \text{Tril}(\mathbf{1}) + (\frac{1}{2} - \frac{1}{\sqrt{2}} \mathbf{1}) \mathbf{I}$  is determined so that the metric is trivialized at  $\boldsymbol{\eta}_0$ , and  $\text{Tril}(\mathbf{1})$  denotes a lower-triangular matrix of ones.

Recall that  $\boldsymbol{\tau} = \mathbf{A}_0 \text{Exp}(\mathbf{D} \odot \boldsymbol{\eta}) \text{Exp}^T(\mathbf{D} \odot \boldsymbol{\eta}) \mathbf{A}_0^T = \mathbf{A}_1 \text{Exp}(\mathbf{D} \odot \boldsymbol{\xi}) \text{Exp}^T(\mathbf{D} \odot \boldsymbol{\xi}) \mathbf{A}_1^T$ . Thus, we have

$$\text{Exp}(\mathbf{D} \odot \boldsymbol{\eta}) \text{Exp}^T(\mathbf{D} \odot \boldsymbol{\eta}) = \text{Exp}(-\mathbf{D} \odot \mathbf{m}) \text{Exp}(\mathbf{D} \odot \boldsymbol{\xi}) \text{Exp}^T(\mathbf{D} \odot \boldsymbol{\xi}) \text{Exp}^T(-\mathbf{D} \odot \mathbf{m}).$$

Since  $\boldsymbol{\eta}$ ,  $\mathbf{m}$  and  $\boldsymbol{\xi}$  are lower-triangular,  $\text{Exp}(\mathbf{D} \odot \boldsymbol{\eta})$ ,  $\text{Exp}(-\mathbf{D} \odot \mathbf{m})$ , and  $\text{Exp}(\mathbf{D} \odot \boldsymbol{\xi})$  are also lower-triangular. Moreover, all the eigenvalues of  $\text{Exp}(\mathbf{D} \odot \boldsymbol{\eta})$ ,  $\text{Exp}(-\mathbf{D} \odot \mathbf{m})$ , and  $\text{Exp}(\mathbf{D} \odot \boldsymbol{\xi})$  are positive.

Note that we make use of the uniqueness of the Cholesky decomposition since  $\text{Exp}(\mathbf{D} \odot \boldsymbol{\eta})$  can be viewed as a Cholesky factor. Thus,  $\text{Exp}(\mathbf{D} \odot \boldsymbol{\eta}) = \text{Exp}(-\mathbf{D} \odot \mathbf{m}) \text{Exp}(\mathbf{D} \odot \boldsymbol{\xi})$ .

By the Baker-Campbell-Hausdorff formula, we have

$$\text{Exp}^{-1}(\text{Exp}(\mathbf{M}) \text{Exp}(\mathbf{N})) = \mathbf{M} + \mathbf{N} + \frac{1}{2} \langle \mathbf{M}, \mathbf{N} \rangle + O(\langle \langle \mathbf{M}, \mathbf{N} \rangle \rangle) + O(\mathbf{N}^2),$$

where  $\langle \mathbf{M}, \mathbf{N} \rangle = \mathbf{M}\mathbf{N} - \mathbf{N}\mathbf{M}$  is the Lie bracket. Thus, we have

$$\boldsymbol{\eta} = (\mathbf{D} \odot \boldsymbol{\xi} - \mathbf{D} \odot \mathbf{m} + \frac{1}{2} \langle -\mathbf{D} \odot \mathbf{m}, \mathbf{D} \odot \boldsymbol{\xi} \rangle) \oslash \mathbf{D} + O(\langle \langle \mathbf{m}, \mathbf{m}, \boldsymbol{\xi} \rangle \rangle) + O(\boldsymbol{\xi}^2),$$

where  $\oslash$  denotes elementwise division.

We get rid of the higher order term  $O(\boldsymbol{\xi}^2)$  by evaluating  $\boldsymbol{\xi} = \boldsymbol{\xi}_0 = \mathbf{0}$ . Recall that  $\mathbf{m} = \mathbf{w}$ . The vector-Jacobian product can be simplified as

$$\begin{aligned} \mathbf{w}^T \mathbf{J}(\boldsymbol{\xi}_0) &= \mathbf{m}^T \left[ \frac{\partial \boldsymbol{\eta}}{\partial \boldsymbol{\xi}} \Big|_{\boldsymbol{\xi}=\boldsymbol{\xi}_0} \right] \\ &= \nabla_{\boldsymbol{\xi}} \text{Tr}(\mathbf{m}^T \boldsymbol{\eta}) \Big|_{\boldsymbol{\xi}=\boldsymbol{\xi}_0} \\ &= \nabla_{\boldsymbol{\xi}} \text{Tr}(\mathbf{m}^T (\mathbf{D} \odot \boldsymbol{\xi} - \mathbf{D} \odot \mathbf{m} + \frac{1}{2} \langle -\mathbf{D} \odot \mathbf{m}, \mathbf{D} \odot \boldsymbol{\xi} \rangle \oslash \mathbf{D}) + O(\langle \langle \mathbf{m}, \mathbf{m}, \boldsymbol{\xi} \rangle \rangle)) \Big|_{\boldsymbol{\xi}=\boldsymbol{\xi}_0} \\ &= \nabla_{\boldsymbol{\xi}} \text{Tr}((\mathbf{m} \oslash \mathbf{D})^T (\mathbf{D} \odot \boldsymbol{\xi} - \mathbf{D} \odot \mathbf{m} + \frac{1}{2} \langle -\mathbf{D} \odot \mathbf{m}, \mathbf{D} \odot \boldsymbol{\xi} \rangle + O(\langle \langle \mathbf{m}, \mathbf{m}, \boldsymbol{\xi} \rangle \rangle))) \Big|_{\boldsymbol{\xi}=\boldsymbol{\xi}_0} \\ &= \underbrace{\mathbf{m}}_{O(\beta)} + \frac{1}{2} \mathbf{D} \odot \underbrace{\langle (-\mathbf{D} \odot \mathbf{m})^T, \mathbf{m} \oslash \mathbf{D} \rangle}_{O(\beta^2)} + \underbrace{O(\langle \langle \mathbf{m}, \mathbf{m}, \mathbf{m}^T \rangle \rangle)}_{O(\beta^3)}. \end{aligned} \quad (32)$$

## E. Simplification of the Metric Calculation at $\boldsymbol{\eta}_0$

Consider  $\boldsymbol{\tau} = \boldsymbol{\phi}_{\boldsymbol{\tau}^{(\text{cur})}}(\boldsymbol{\eta}) = \mathbf{A}\mathbf{A}^T \in S_{++}^{k \times k}$ , where  $\mathbf{A} = \mathbf{A}^{(\text{cur})} \text{Exp}(\mathbf{D} \odot \boldsymbol{\eta})$ .

For notation simplicity, we let  $\mathbf{A}_0 = \mathbf{A}^{(\text{cur})}$  and  $\boldsymbol{\tau}_0 = \boldsymbol{\tau}^{(\text{cur})} = \mathbf{A}_0 \mathbf{A}_0^T$ . Let  $\tilde{\boldsymbol{\eta}}$  denote the vector representation of the learnable part of  $\boldsymbol{\eta}$ . By definition of the affine invariant metric, we have

$$\begin{aligned} \mathbf{F}(\boldsymbol{\eta}_0) &= -2 \mathbb{E}_{\mathcal{N}(\mathbf{0}, \boldsymbol{\tau})} \left[ \nabla_{\tilde{\boldsymbol{\eta}}}^2 \log \mathcal{N}(\mathbf{0}, \boldsymbol{\tau}) \right] \Big|_{\boldsymbol{\eta}=\boldsymbol{\eta}_0} \\ &= \mathbb{E}_{\mathcal{N}(\mathbf{0}, \boldsymbol{\tau})} \left[ \nabla_{\tilde{\boldsymbol{\eta}}}^2 \left\{ \text{Tr}[\mathbf{x}\mathbf{x}^T \mathbf{A}_0^{-T} \text{Exp}^T(-\mathbf{D} \odot \boldsymbol{\eta}) \text{Exp}(-\mathbf{D} \odot \boldsymbol{\eta}) \mathbf{A}_0^{-1}] + 2 \log \det \text{Exp}(\mathbf{D} \odot \boldsymbol{\eta}) \right\} \right] \Big|_{\boldsymbol{\eta}=\boldsymbol{\eta}_0} \\ &= \nabla_{\tilde{\boldsymbol{\eta}}}^2 \left\{ \text{Tr}[\mathbb{E}_{\mathcal{N}(\mathbf{0}, \boldsymbol{\tau}_0)}[\mathbf{x}\mathbf{x}^T] \mathbf{A}_0^{-T} \text{Exp}^T(-\mathbf{D} \odot \boldsymbol{\eta}) \text{Exp}(-\mathbf{D} \odot \boldsymbol{\eta}) \mathbf{A}_0^{-1}] + 2 \log \det \text{Exp}(\mathbf{D} \odot \boldsymbol{\eta}) \right\} \Big|_{\boldsymbol{\eta}=\boldsymbol{\eta}_0} \\ &= \nabla_{\tilde{\boldsymbol{\eta}}}^2 \left\{ \text{Tr}[\mathbf{A}_0 \mathbf{A}_0^T] \mathbf{A}_0^{-T} \text{Exp}^T(-\mathbf{D} \odot \boldsymbol{\eta}) \text{Exp}(-\mathbf{D} \odot \boldsymbol{\eta}) \mathbf{A}_0^{-1} + 2 \log \det \text{Exp}(\mathbf{D} \odot \boldsymbol{\eta}) \right\} \Big|_{\boldsymbol{\eta}=\boldsymbol{\eta}_0} \\ &= \nabla_{\tilde{\boldsymbol{\eta}}}^2 \left\{ \text{Tr}[\text{Exp}^T(-\mathbf{D} \odot \boldsymbol{\eta}) \text{Exp}(-\mathbf{D} \odot \boldsymbol{\eta})] + 2 \log \det \text{Exp}(\mathbf{D} \odot \boldsymbol{\eta}) \right\} \Big|_{\boldsymbol{\eta}=\boldsymbol{\eta}_0} \\ &= \nabla_{\tilde{\boldsymbol{\eta}}}^2 \left\{ \text{Tr}[\text{Exp}^T(-\mathbf{D} \odot \boldsymbol{\eta}) \text{Exp}(-\mathbf{D} \odot \boldsymbol{\eta})] + 2 \text{Tr}[\mathbf{D} \odot \boldsymbol{\eta}] \right\} \Big|_{\boldsymbol{\eta}=\boldsymbol{\eta}_0} \quad (\text{ignore linear terms for a 2nd order derivative}) \\ &= \nabla_{\tilde{\boldsymbol{\eta}}}^2 \left\{ \text{Tr}[\text{Exp}^T(-\mathbf{D} \odot \boldsymbol{\eta}) \text{Exp}(-\mathbf{D} \odot \boldsymbol{\eta})] \right\} \Big|_{\boldsymbol{\eta}=\boldsymbol{\eta}_0}. \end{aligned} \quad (33)$$

Note that we express  $\text{Exp}(-\mathbf{D} \odot \boldsymbol{\eta})$  as  $\text{Exp}(-\mathbf{D} \odot \boldsymbol{\eta}) = \mathbf{I} - \mathbf{D} \odot \boldsymbol{\eta} + \frac{1}{2}(\mathbf{D} \odot \boldsymbol{\eta})^2 + O(\boldsymbol{\eta}^3)$ . Since we evaluate the metric at  $\boldsymbol{\eta}_0 = \mathbf{0}$ , we can get rid of the higher order term  $O(\boldsymbol{\eta}^3)$ , which leads to the following simplification,

$$\begin{aligned} & \nabla_{\eta_{ij}} \text{Tr}[\text{Exp}^T(-\mathbf{D} \odot \boldsymbol{\eta}) \text{Exp}(-\mathbf{D} \odot \boldsymbol{\eta})] \\ &= 2\text{Tr}[\text{Exp}(-\mathbf{D} \odot \boldsymbol{\eta}) [\nabla_{\eta_{ij}} \text{Exp}^T(-\mathbf{D} \odot \boldsymbol{\eta})]] \\ &= 2D_{ij} \nabla_{\eta_{ij}} \left\{ \text{Tr}[\text{Exp}(-\mathbf{D} \odot \boldsymbol{\eta}) [-\mathbf{E}_{ij} + \frac{1}{2}\mathbf{E}_{ij}(\mathbf{D} \odot \boldsymbol{\eta}) + \frac{1}{2}(\mathbf{D} \odot \boldsymbol{\eta})\mathbf{E}_{ij} + O(\boldsymbol{\eta}^2)]^T] \right\}. \end{aligned}$$

Thus, we have

$$\begin{aligned} & \nabla_{\boldsymbol{\eta}} \text{Tr}[\text{Exp}^T(-\mathbf{D} \odot \boldsymbol{\eta}) \text{Exp}(-\mathbf{D} \odot \boldsymbol{\eta})] \\ &= \mathbf{D} \odot [-2\text{Exp}(-\mathbf{D} \odot \boldsymbol{\eta}) + \text{Exp}(-\mathbf{D} \odot \boldsymbol{\eta})(\mathbf{D} \odot \boldsymbol{\eta})^T + (\mathbf{D} \odot \boldsymbol{\eta})^T \text{Exp}(-\mathbf{D} \odot \boldsymbol{\eta})] + O(\boldsymbol{\eta}^2). \end{aligned}$$

To show  $\mathbf{F}(\boldsymbol{\eta}_0) = \mathbf{I}$ , we show that  $\mathbf{F}(\boldsymbol{\eta}_0)\mathbf{v} = \mathbf{v}$  for any  $\mathbf{v}$ . Let  $\mathbf{V}$  be the matrix representation of  $\mathbf{v}$ , which has the same structure as  $\boldsymbol{\eta}$ , such as being symmetric or being lower-triangular. Then,

$$\begin{aligned} & \mathbf{F}(\boldsymbol{\eta}_0)\mathbf{v} \\ &= \nabla_{\tilde{\boldsymbol{\eta}}}^2 \left\{ \text{Tr}[\text{Exp}^T(-\mathbf{D} \odot \boldsymbol{\eta}) \text{Exp}(-\mathbf{D} \odot \boldsymbol{\eta})] \right\} \Big|_{\boldsymbol{\eta}=\boldsymbol{\eta}_0} \mathbf{v} \\ &= \nabla_{\tilde{\boldsymbol{\eta}}} \left\{ \mathbf{v}^T \nabla_{\tilde{\boldsymbol{\eta}}} \text{Tr}[\text{Exp}^T(-\mathbf{D} \odot \boldsymbol{\eta}) \text{Exp}(-\mathbf{D} \odot \boldsymbol{\eta})] \right\} \Big|_{\boldsymbol{\eta}=\boldsymbol{\eta}_0}, \quad (\text{note: } \tilde{\boldsymbol{\eta}}, \mathbf{v} \text{ are vectors}) \\ &= \nabla_{\tilde{\boldsymbol{\eta}}} \text{Tr} \left\{ \mathbf{V}^T \nabla_{\boldsymbol{\eta}} \text{Tr}[\text{Exp}^T(-\mathbf{D} \odot \boldsymbol{\eta}) \text{Exp}(-\mathbf{D} \odot \boldsymbol{\eta})] \right\} \Big|_{\boldsymbol{\eta}=\boldsymbol{\eta}_0} \quad (\text{note: } \boldsymbol{\eta}, \mathbf{V} \text{ are matrices}) \\ &= \nabla_{\tilde{\boldsymbol{\eta}}} \text{Tr} \left\{ \mathbf{V}^T (\mathbf{D} \odot [-2\text{Exp}(-\mathbf{D} \odot \boldsymbol{\eta}) + \text{Exp}(-\mathbf{D} \odot \boldsymbol{\eta})(\mathbf{D} \odot \boldsymbol{\eta})^T + (\mathbf{D} \odot \boldsymbol{\eta})^T \text{Exp}(-\mathbf{D} \odot \boldsymbol{\eta})] + O(\boldsymbol{\eta}^2)) \right\} \Big|_{\boldsymbol{\eta}=\boldsymbol{\eta}_0}. \end{aligned}$$

We can get rid of the higher-order term  $O(\boldsymbol{\eta}^2)$  by evaluating  $\boldsymbol{\eta} = \boldsymbol{\eta}_0 = \mathbf{0}$  and noting that

$$\text{Tr}(\mathbf{A}^T (\mathbf{D} \odot \mathbf{B})) = \sum (\mathbf{A} \odot (\mathbf{D} \odot \mathbf{B})) = \text{Tr}((\mathbf{D} \odot \mathbf{A})^T \mathbf{B}).$$

Also note that

$$\begin{aligned} & \nabla_{\eta_{ij}} \text{Tr} \left\{ (\mathbf{D} \odot \mathbf{V})^T [-2\text{Exp}(-\mathbf{D} \odot \boldsymbol{\eta}) + \text{Exp}(-\mathbf{D} \odot \boldsymbol{\eta})(\mathbf{D} \odot \boldsymbol{\eta})^T + (\mathbf{D} \odot \boldsymbol{\eta})^T \text{Exp}(-\mathbf{D} \odot \boldsymbol{\eta})] \right\} \Big|_{\boldsymbol{\eta}=\boldsymbol{\eta}_0} \\ &= \text{Tr} \left\{ (\mathbf{D} \odot \mathbf{V})^T 2D_{ij} [\mathbf{E}_{ij} + \mathbf{E}_{ij}^T] \right\} \Big|_{\boldsymbol{\eta}=\boldsymbol{\eta}_0}. \end{aligned}$$

Thus, we have

$$\begin{aligned} & \nabla_{\boldsymbol{\eta}} \text{Tr} \left\{ (\mathbf{D} \odot \mathbf{V})^T [-2\text{Exp}(-\mathbf{D} \odot \boldsymbol{\eta}) + \text{Exp}(-\mathbf{D} \odot \boldsymbol{\eta})(\mathbf{D} \odot \boldsymbol{\eta})^T + (\mathbf{D} \odot \boldsymbol{\eta})^T \text{Exp}(-\mathbf{D} \odot \boldsymbol{\eta})] \right\} \Big|_{\boldsymbol{\eta}=\boldsymbol{\eta}_0} \\ &= 2\mathbf{D} \odot (\mathbf{D} \odot \mathbf{V} + (\mathbf{D} \odot \mathbf{V})^T). \end{aligned}$$

### E.1. Symmetric Cases

When  $\boldsymbol{\eta}$  is symmetric,  $\mathbf{V}$  is also symmetric so

$$\begin{aligned} & \mathbf{F}(\boldsymbol{\eta}_0)\mathbf{v} \\ &= \nabla_{\tilde{\boldsymbol{\eta}}} \text{Tr} \left\{ \mathbf{V}^T (\mathbf{D} \odot [-2\text{Exp}(-\mathbf{D} \odot \boldsymbol{\eta}) + \text{Exp}(-\mathbf{D} \odot \boldsymbol{\eta})(\mathbf{D} \odot \boldsymbol{\eta})^T + (\mathbf{D} \odot \boldsymbol{\eta})^T \text{Exp}(-\mathbf{D} \odot \boldsymbol{\eta})] + O(\boldsymbol{\eta}^2)) \right\} \Big|_{\boldsymbol{\eta}=\boldsymbol{\eta}_0} \\ &= \text{vech}(2\mathbf{D} \odot (\mathbf{D} \odot \mathbf{V} + \mathbf{D} \odot \mathbf{V})) = 4\text{vech}(\mathbf{D}^2 \odot \mathbf{V}). \end{aligned}$$

When  $\mathbf{D} = \frac{1}{2}\mathbf{1}$ , we have  $4\text{vech}(\mathbf{D}^2 \odot \mathbf{V}) = \text{vech}(\mathbf{V})$ , where  $\mathbf{1}$  is a matrix of ones. Thus,  $\mathbf{F}(\boldsymbol{\eta}_0) = \mathbf{I}$ .

### E.2. Triangular Cases

Without loss of generality, we assume that  $\boldsymbol{\eta}$  is lower-triangular, in which case  $\mathbf{V}$  is lower-triangular, and thus

$$\begin{aligned} & \mathbf{F}(\boldsymbol{\eta}_0)\mathbf{v} \\ &= \nabla_{\tilde{\boldsymbol{\eta}}} \text{Tr} \left\{ \mathbf{V}^T (\mathbf{D} \odot [-2\text{Exp}(-\mathbf{D} \odot \boldsymbol{\eta}) + \text{Exp}(-\mathbf{D} \odot \boldsymbol{\eta})(\mathbf{D} \odot \boldsymbol{\eta})^T + (\mathbf{D} \odot \boldsymbol{\eta})^T \text{Exp}(-\mathbf{D} \odot \boldsymbol{\eta})] + O(\boldsymbol{\eta}^2)) \right\} \Big|_{\boldsymbol{\eta}=\boldsymbol{\eta}_0} \\ &= \text{tril}(2\mathbf{D} \odot (\mathbf{D} \odot \mathbf{V} + \mathbf{D} \odot \mathbf{V}^T)) \quad (\mathbf{V}^T \text{ is upper-triangular. Thus } \text{tril}(\mathbf{V}^T) = \text{Diag}(\mathbf{V}^T) = \text{Diag}(\mathbf{V})) \\ &= \text{tril}(2\mathbf{D}^2 \odot (\mathbf{V} + \text{Diag}(\mathbf{V}))), \end{aligned}$$

where  $\text{tril}(\cdot)$  represents a vector representation of the learnable part of a lower-triangular matrix and  $\text{Tril}(\cdot)$  denotes a lower-triangular matrix.

When  $\mathbf{D} = \frac{1}{\sqrt{2}}\text{Tril}(\mathbf{1}) + (\frac{1}{2} - \frac{1}{\sqrt{2}}\mathbf{I})$ , we have  $\text{tril}(2\mathbf{D}^2 \odot (\mathbf{V} + \text{Diag}(\mathbf{V}))) = \text{tril}(\mathbf{V})$ , where  $\text{Tril}(\mathbf{1})$  is a lower-triangular matrix of ones. Thus,  $\mathbf{F}(\boldsymbol{\eta}_0) = \mathbf{I}$ .

## F. An Accurate Approximation of the Euclidean Transport Map

We consider the first-order approximation of the Euclidean transport

$$\mathbf{m}^{(\eta_1)} = T_{\eta_0 \rightarrow \eta_1}(\mathbf{m}^{(\eta_0)}) = \boldsymbol{\omega}(1) \approx \underbrace{\boldsymbol{\omega}(0)}_{\mathbf{m}^{(\eta_0)}} + \dot{\boldsymbol{\omega}}(0), \quad (34)$$

where we have to evaluate the Christoffel symbols as discussed below.

By the transport ODE in Eq. (27), we can compute  $\dot{\boldsymbol{\omega}}(0)$  via

$$\dot{\omega}_c(0) - \sum_{a,b} \Gamma_{cb}^a(\mathbf{r}(0)) \omega_a(0) \dot{r}^b(0) = 0,$$

where  $\mathbf{r}(0) = \boldsymbol{\eta}_0$  is the current point and  $\dot{\mathbf{r}}(0)$  is the Riemannian gradient so that  $\boldsymbol{\eta}_1 = \text{RExp}(\boldsymbol{\eta}_0, \dot{\mathbf{r}}(0))$ . In our case, as shown in Eq. (8),  $\dot{\mathbf{r}}(0) = -\mathbf{F}^{-1}(\boldsymbol{\eta}_0)\mathbf{m}^{(\eta_0)} = \mathbf{m}^{(\eta_0)}$  and  $\boldsymbol{\omega}(0) = \mathbf{m}^{(\eta_0)}$ .

Note that the metric and Christoffel symbols are evaluated at  $\boldsymbol{\eta}_0 = \mathbf{0}$ . The computation can be simplified due to the trivialized metric as  $\mathbf{F}^{-1}(\boldsymbol{\eta}_0) = \mathbf{I}$  and

$$\Gamma_{cb}^a(\boldsymbol{\eta}_0) = \sum_d F^{ad}(\boldsymbol{\eta}_0) \Gamma_{d,cb}(\boldsymbol{\eta}_0) = \sum_d \delta^{ad} \frac{1}{2} [\partial_c F_{bd}(\boldsymbol{\eta}_0) + \partial_b F_{cd}(\boldsymbol{\eta}_0) - \partial_d F_{cb}(\boldsymbol{\eta}_0)],$$

where  $F^{ad}(\boldsymbol{\eta}_0) = \delta^{ad}$ . Thus, we have the following simplification,

$$\begin{aligned} \dot{\omega}_c(0) &= -\frac{1}{2} \sum_{b,d} [\partial_c F_{bd}(\boldsymbol{\eta}_0) + \partial_b F_{cd}(\boldsymbol{\eta}_0) - \partial_d F_{cb}(\boldsymbol{\eta}_0)] (\mathbf{m}^{(\eta_0)})^d (\mathbf{m}^{(\eta_0)})^b \\ &= -\frac{1}{2} \sum_{b,d} \partial_c F_{bd}(\boldsymbol{\eta}_0) (\mathbf{m}^{(\eta_0)})^d (\mathbf{m}^{(\eta_0)})^b. \end{aligned}$$

For notation simplicity, we let  $\mathbf{m} = \mathbf{m}^{(\eta_0)}$  and  $\mathbf{A}_0 = \mathbf{A}^{(\text{cur})}$ .

For normal coordinate  $\mathbf{A} = \mathbf{A}_0 \text{Exp}_m(\mathbf{D} \odot \boldsymbol{\eta})$ , we can obtain the following result. The calculation is similar to the metric calculation in Appx. E.

$$\dot{\boldsymbol{\omega}}(0) = \underbrace{\mathbf{D} \odot \left( \left\langle \mathbf{D} \odot \mathbf{m}, (\mathbf{D} \odot \mathbf{m})^T \right\rangle \right)}_{O(\beta^2)}, \quad (35)$$

where  $\langle \mathbf{N}, \mathbf{M} \rangle := \mathbf{NM} - \mathbf{MN}$  is the Lie bracket, the  $\beta$  is the stepsize used in Eq. (8).

When  $\boldsymbol{\eta}$  is symmetric, we know that  $\mathbf{m}$  is symmetric. Thus, we have  $\dot{\boldsymbol{\omega}}(0) = \mathbf{0}$ .

## G. Structured NGD as a Special Case

### G.1. Normal Coordinate for Structured NGD

We can obtain coordinate (13) from coordinate (12).

In Eq. (12), the normal coordinate is defined as  $\mathbf{A} = \mathbf{A}_0 \text{Exp}_m \left( \begin{bmatrix} \frac{1}{2} \boldsymbol{\eta}_L & \frac{1}{\sqrt{2}} \boldsymbol{\eta}_\mu \\ \mathbf{0} & 0 \end{bmatrix} \right)$ , where we use  $\mathbf{A}_0$  to denote  $\mathbf{A}^{(\text{cur})}$ .

Note that

$$\text{Exp}_m \left( \begin{bmatrix} \frac{1}{2} \boldsymbol{\eta}_L & \frac{1}{\sqrt{2}} \boldsymbol{\eta}_\mu \\ \mathbf{0} & 0 \end{bmatrix} \right) = \begin{bmatrix} \text{Exp}_m(\frac{1}{2} \boldsymbol{\eta}_L) & \frac{1}{\sqrt{2}} \boldsymbol{\eta}_\mu + O(\boldsymbol{\eta}_L \boldsymbol{\eta}_\mu) \\ \mathbf{0} & 1 \end{bmatrix}.$$

The main point is that  $O(\boldsymbol{\eta}_L \boldsymbol{\eta}_\mu)$  vanishes in the metric computation since we evaluate the metric at  $\boldsymbol{\eta}_0 = \{\boldsymbol{\eta}_L, \boldsymbol{\eta}_\mu\} = \mathbf{0}$ . Thus, we can ignore  $O(\boldsymbol{\eta}_L \boldsymbol{\eta}_\mu)$ , which leads another normal coordinate.

By ignoring  $O(\boldsymbol{\eta}_L \boldsymbol{\eta}_\mu)$ , we recover Eq. (13):

$$\mathbf{A} = \mathbf{A}_0 \begin{bmatrix} \text{Exp}\left(\frac{1}{2}\boldsymbol{\eta}_L\right) & \frac{1}{\sqrt{2}}\boldsymbol{\eta}_\mu \\ \mathbf{0} & 1 \end{bmatrix} = \begin{bmatrix} \mathbf{L}_0 & \boldsymbol{\mu}_0 \\ \mathbf{0} & 1 \end{bmatrix} \begin{bmatrix} \text{Exp}\left(\frac{1}{2}\boldsymbol{\eta}_L\right) & \frac{1}{\sqrt{2}}\boldsymbol{\eta}_\mu \\ \mathbf{0} & 1 \end{bmatrix} = \begin{bmatrix} \mathbf{L}_0 \text{Exp}\left(\frac{1}{2}\boldsymbol{\eta}_L\right) & \boldsymbol{\mu}_0 + \frac{1}{\sqrt{2}}\mathbf{L}_0\boldsymbol{\eta}_\mu \\ \mathbf{0} & 1 \end{bmatrix}. \quad (36)$$

To show that  $O(\boldsymbol{\eta}_L \boldsymbol{\eta}_\mu)$  vanishes in the metric computation, we have to show all cross terms between  $\boldsymbol{\eta}_L$  and  $\boldsymbol{\eta}_\mu$  of the metric vanish. Using Eq. (33),

$$\begin{aligned} & \mathbb{E}_{\mathcal{N}(\mathbf{0}, \boldsymbol{\tau})} [\nabla_{\boldsymbol{\eta}_{L_{jk}}} \nabla_{\boldsymbol{\eta}_{\mu_i}} \log \mathcal{N}(\mathbf{0}, \boldsymbol{\tau})] \Big|_{\boldsymbol{\eta}=\boldsymbol{\eta}_0} \\ &= \nabla_{\boldsymbol{\eta}_{L_{jk}}} \nabla_{\boldsymbol{\eta}_{\mu_i}} \left\{ \text{Tr} \left[ \text{Exp}\left(-\begin{bmatrix} \frac{1}{2}\boldsymbol{\eta}_L & \frac{1}{\sqrt{2}}\boldsymbol{\eta}_\mu \\ \mathbf{0} & 0 \end{bmatrix}\right) \text{Exp}\left(-\begin{bmatrix} \frac{1}{2}\boldsymbol{\eta}_L & \frac{1}{\sqrt{2}}\boldsymbol{\eta}_\mu \\ \mathbf{0} & 0 \end{bmatrix}\right) \right] \right\} \Big|_{\boldsymbol{\eta}=\boldsymbol{\eta}_0}. \end{aligned}$$

We can drop higher order terms since we evaluate at  $\boldsymbol{\eta}_0 = \{\boldsymbol{\eta}_L, \boldsymbol{\eta}_\mu\} = \mathbf{0}$ . We get

$$\begin{aligned} & \nabla_{\boldsymbol{\eta}_{L_{jk}}} \nabla_{\boldsymbol{\eta}_{\mu_i}} \left\{ \text{Tr} \left[ \text{Exp}\left(-\begin{bmatrix} \frac{1}{2}\boldsymbol{\eta}_L & \frac{1}{\sqrt{2}}\boldsymbol{\eta}_\mu \\ \mathbf{0} & 0 \end{bmatrix}\right) \text{Exp}\left(-\begin{bmatrix} \frac{1}{2}\boldsymbol{\eta}_L & \frac{1}{\sqrt{2}}\boldsymbol{\eta}_\mu \\ \mathbf{0} & 0 \end{bmatrix}\right) \right] \right\} \\ &= 2\nabla_{\boldsymbol{\eta}_{L_{jk}}} \left\{ \text{Tr} \left[ \left\{ \nabla_{\boldsymbol{\eta}_{\mu_i}} \text{Exp}\left(-\begin{bmatrix} \frac{1}{2}\boldsymbol{\eta}_L & \frac{1}{\sqrt{2}}\boldsymbol{\eta}_\mu \\ \mathbf{0} & 0 \end{bmatrix}\right) \right\} \text{Exp}\left(-\begin{bmatrix} \frac{1}{2}\boldsymbol{\eta}_L & \frac{1}{\sqrt{2}}\boldsymbol{\eta}_\mu \\ \mathbf{0} & 0 \end{bmatrix}\right) \right] \right\} \\ &= 2\nabla_{\boldsymbol{\eta}_{L_{jk}}} \text{Tr} \left[ \left( -\begin{bmatrix} \mathbf{0} & \frac{1}{\sqrt{2}}\mathbf{e}_i \\ \mathbf{0} & 0 \end{bmatrix} + \frac{1}{2} \begin{bmatrix} \mathbf{0} & \frac{1}{\sqrt{2}}\mathbf{e}_i \\ \mathbf{0} & 0 \end{bmatrix} \begin{bmatrix} \frac{1}{2}\boldsymbol{\eta}_L & \frac{1}{\sqrt{2}}\boldsymbol{\eta}_\mu \\ \mathbf{0} & 0 \end{bmatrix} + \frac{1}{2} \begin{bmatrix} \frac{1}{2}\boldsymbol{\eta}_L & \frac{1}{\sqrt{2}}\boldsymbol{\eta}_\mu \\ \mathbf{0} & 0 \end{bmatrix} \begin{bmatrix} \mathbf{0} & \frac{1}{\sqrt{2}}\mathbf{e}_i \\ \mathbf{0} & 0 \end{bmatrix} \right)^T \text{Exp}\left(-\begin{bmatrix} \frac{1}{2}\boldsymbol{\eta}_L & \frac{1}{\sqrt{2}}\boldsymbol{\eta}_\mu \\ \mathbf{0} & 0 \end{bmatrix}\right) \right] \\ &= 2\nabla_{\boldsymbol{\eta}_{L_{jk}}} \text{Tr} \left[ \left( -\begin{bmatrix} \mathbf{0} & \frac{1}{\sqrt{2}}\mathbf{e}_i \\ \mathbf{0} & 0 \end{bmatrix} + \frac{1}{2} \begin{bmatrix} \frac{1}{2}\boldsymbol{\eta}_L & \frac{1}{\sqrt{2}}\boldsymbol{\eta}_\mu \\ \mathbf{0} & 0 \end{bmatrix} \begin{bmatrix} \mathbf{0} & \frac{1}{\sqrt{2}}\mathbf{e}_i \\ \mathbf{0} & 0 \end{bmatrix} \right)^T \text{Exp}\left(-\begin{bmatrix} \frac{1}{2}\boldsymbol{\eta}_L & \frac{1}{\sqrt{2}}\boldsymbol{\eta}_\mu \\ \mathbf{0} & 0 \end{bmatrix}\right) \right] \\ &= 2\text{Tr} \left[ \begin{bmatrix} \mathbf{0} & \frac{1}{\sqrt{2}}\mathbf{e}_i \\ \mathbf{0} & 0 \end{bmatrix}^T \begin{bmatrix} \frac{1}{2}\mathbf{E}_{jk} & \mathbf{0} \\ \mathbf{0} & 0 \end{bmatrix} + \frac{1}{2} \left( \begin{bmatrix} \frac{1}{2}\mathbf{E}_{jk} & \mathbf{0} \\ \mathbf{0} & 0 \end{bmatrix} \begin{bmatrix} \mathbf{0} & \frac{1}{\sqrt{2}}\mathbf{e}_i \\ \mathbf{0} & 0 \end{bmatrix} \right)^T \right] = 0, \end{aligned}$$

and therefore

$$\mathbb{E}_{\mathcal{N}(\mathbf{0}, \boldsymbol{\tau})} [\nabla_{\boldsymbol{\eta}_{L_{jk}}} \nabla_{\boldsymbol{\eta}_{\mu_i}} \log \mathcal{N}(\mathbf{0}, \boldsymbol{\tau})] \Big|_{\boldsymbol{\eta}=\boldsymbol{\eta}_0} = 0.$$

## G.2. Gaussian Identities in Structured NGD

Recall that the manifold is defined as

$$\mathcal{M} = \left\{ \boldsymbol{\tau} = \begin{bmatrix} \mathbf{V} & \boldsymbol{\mu} \\ \boldsymbol{\mu}^T & 1 \end{bmatrix} \in \mathbb{R}^{(d+1) \times (d+1)} \mid \boldsymbol{\tau} \succ 0 \right\}.$$

To use Gaussian gradient identities, we first change the notation to avoid confusion. The manifold is reexpressed as follows, where we change the notation from  $\boldsymbol{\mu}$  to  $\mathbf{m}$ :

$$\mathcal{M} = \left\{ \boldsymbol{\tau} = \begin{bmatrix} \mathbf{V} & \mathbf{m} \\ \mathbf{m}^T & 1 \end{bmatrix} \in \mathbb{R}^{(d+1) \times (d+1)} \mid \boldsymbol{\tau} \succ 0 \right\}.$$

In Sec. 3.3.1, we can compute the Euclidean gradient

$$\mathbf{g}(\boldsymbol{\eta}_0) = \{\mathbf{L}^T \mathbf{g}_1 \mathbf{L}, \sqrt{2}\mathbf{L}^T (\mathbf{g}_1 \mathbf{m} + \mathbf{g}_2)\},$$

where we use our new notation, and where  $\mathbf{g}(\boldsymbol{\tau}^{\text{cur}}) = \begin{bmatrix} \mathbf{g}_1 & \mathbf{g}_2 \\ \mathbf{g}_2^T & 0 \end{bmatrix}$  is a (symmetric) Euclidean gradient w.r.t.  $\boldsymbol{\tau} \in \mathcal{M}$ .

By the chain rule, we have

$$\frac{\partial \ell}{\partial m_i} = \text{Tr} \left( \underbrace{\left( \frac{\partial \ell}{\partial \boldsymbol{\tau}} \right)^T}_{\mathbf{g}^T(\boldsymbol{\tau})} \frac{\partial \boldsymbol{\tau}}{\partial m_i} \right) = \text{Tr} \left( \begin{bmatrix} \mathbf{g}_1 & \mathbf{g}_2 \\ \mathbf{g}_2^T & 0 \end{bmatrix} \begin{bmatrix} \mathbf{0} & \mathbf{e}_i \\ \mathbf{e}_i^T & 1 \end{bmatrix} \right) = 2\mathbf{g}_2^T \mathbf{e}_i,$$

so  $\mathbf{g}_m = \frac{\partial \ell}{\partial \mathbf{m}} = 2\mathbf{g}_2$ . Similarly, we have  $\mathbf{g}_V = \frac{\partial \ell}{\partial \mathbf{V}} = \mathbf{g}_1$ .

Note that in Gaussian cases, we have  $\boldsymbol{\mu} = \mathbf{m}$  and  $\boldsymbol{\Sigma} = \mathbf{V} - \mathbf{m}\mathbf{m}^T$ . Thus, we have

$$\begin{aligned}\nabla_{\mu_i} \ell &= \text{Tr} \left( \left( \frac{\partial \ell}{\partial \mathbf{m}} \right)^T \frac{\partial \mathbf{m}}{\partial \mu_i} \right) + \text{Tr} \left( \left( \frac{\partial \ell}{\partial \mathbf{V}} \right)^T \frac{\partial \mathbf{V}}{\partial \mu_i} \right) = \mathbf{g}_m^T \mathbf{e}_i + \text{Tr} \left( \mathbf{g}_V^T (\mathbf{e}_i \mathbf{m}^T + \mathbf{m} \mathbf{e}_i^T) \right), \\ \nabla_{\Sigma_{jk}} \ell &= \text{Tr} \left( \left( \frac{\partial \ell}{\partial \mathbf{m}} \right)^T \frac{\partial \mathbf{m}}{\partial \Sigma_{jk}} \right) + \text{Tr} \left( \left( \frac{\partial \ell}{\partial \mathbf{V}} \right)^T \frac{\partial \mathbf{V}}{\partial \Sigma_{jk}} \right) = 0 + \text{Tr} \left( \mathbf{g}_V^T \mathbf{E}_{jk} \right),\end{aligned}\quad (37)$$

which implies that

$$\begin{aligned}\mathbf{g}_\mu &= \mathbf{g}_m + (\mathbf{g}_V + \mathbf{g}_V^T) \mathbf{m} = \mathbf{g}_m + 2\mathbf{g}_V \mathbf{m} = 2\mathbf{g}_2 + 2\mathbf{g}_1 \boldsymbol{\mu}, \\ \mathbf{g}_\Sigma &= \mathbf{g}_V = \mathbf{g}_1.\end{aligned}$$

Thus  $\mathbf{g}_1$  and  $\mathbf{g}_2$  can be reexpressed using Gaussian gradients  $\mathbf{g}_\mu$  and  $\mathbf{g}_\Sigma$  as  $\mathbf{g}_1 = \mathbf{g}_\Sigma$  and  $\mathbf{g}_2 = \frac{1}{2}(\mathbf{g}_\mu - 2\mathbf{g}_\Sigma \boldsymbol{\mu})$ .

## H. SPD Manifolds

### H.1. Generalized Normal Coordinates

We first show that the local coordinate  $\boldsymbol{\tau} = \boldsymbol{\phi}_{\boldsymbol{\tau}^{(\text{cur})}}(\boldsymbol{\eta}) = \mathbf{A}\mathbf{A}^T$  is a generalized normal coordinate defined at the reference point  $\boldsymbol{\tau}^{(\text{cur})} = \mathbf{A}^{(\text{cur})}(\mathbf{A}^{(\text{cur})})^T$ , where  $\boldsymbol{\eta} \in \mathbb{R}^{k \times k}$  is symmetric, and  $\mathbf{A} = \mathbf{A}^{(\text{cur})} \text{ExpM}(\frac{1}{2}\boldsymbol{\eta})$ .

It is easy to verify that Assumption 1 holds since  $\boldsymbol{\phi}_{\boldsymbol{\tau}^{(\text{cur})}}(\boldsymbol{\eta}_0) = \boldsymbol{\tau}^{(\text{cur})}$  at  $\boldsymbol{\eta}_0 = \mathbf{0}$ .

As shown in Appx. E.1, the metric is trivialized at  $\boldsymbol{\eta}_0 = \mathbf{0}$ . Thus, Assumption 2 holds.

Recall that the standard normal coordinate is  $\boldsymbol{\tau} = \boldsymbol{\psi}_{\boldsymbol{\tau}^{(\text{cur})}}(\boldsymbol{\eta}) = (\boldsymbol{\tau}^{(\text{cur})})^{1/2} \text{ExpM}(\boldsymbol{\eta}) (\boldsymbol{\tau}^{(\text{cur})})^{1/2}$ , where Assumption 3 holds. Our generalized normal coordinate is defined as  $\boldsymbol{\tau} = \boldsymbol{\psi}_{\boldsymbol{\tau}^{(\text{cur})}}(\boldsymbol{\eta}) = \mathbf{A}^{(\text{cur})} \text{ExpM}(\boldsymbol{\eta}) (\mathbf{A}^{(\text{cur})})^T$ , where  $\boldsymbol{\eta}$  is symmetric. The only difference between these two coordinates is a multiplicative constant. Differentiability and smoothness remain the same. The injectivity is due to the uniqueness of the symmetric square root of a matrix. This statement is also valid when  $\boldsymbol{\tau}$  is a triangular matrix due to the uniqueness of the Cholesky decomposition. Thus, Assumption 3 holds in our generalized normal coordinate.

For any symmetric  $\boldsymbol{\eta} \in \mathbb{R}^{k \times k}$ , the space of  $\boldsymbol{\eta}$  is a (abstract) vector space since scalar products and matrix additions are also symmetric. Thus, Assumption 4 holds.

### H.2. Euclidean Gradients in Normal Coordinates

As mentioned in Sec. 3.2, there are many generalized normal coordinates such as

- $\boldsymbol{\phi}_{\boldsymbol{\tau}^{(\text{cur})}}(\boldsymbol{\eta}) = \mathbf{A}\mathbf{A}^T$ , where  $\boldsymbol{\eta}$  is symmetric,  $\mathbf{A} := \mathbf{A}^{(\text{cur})} \text{ExpM}(\frac{1}{2}\boldsymbol{\eta})$ ,
- $\boldsymbol{\phi}_{\boldsymbol{\tau}^{(\text{cur})}}(\boldsymbol{\eta}) = \mathbf{B}^{-T} \mathbf{B}^{-1}$ , where  $\boldsymbol{\eta}$  is symmetric,  $\mathbf{B} := \mathbf{B}^{(\text{cur})} \text{ExpM}(-\frac{1}{2}\boldsymbol{\eta})$ ,
- $\boldsymbol{\phi}_{\boldsymbol{\tau}^{(\text{cur})}}(\boldsymbol{\eta}) = \mathbf{C}^T \mathbf{C}$ , where  $\boldsymbol{\eta}$  is symmetric,  $\mathbf{C} := \text{ExpM}(\frac{1}{2}\boldsymbol{\eta}) \mathbf{C}^{(\text{cur})}$ .

We show how to compute the Euclidean gradient  $\mathbf{g}(\boldsymbol{\eta}_0)$  needed in Eq. (8), where we assume that the Euclidean gradient  $\nabla_{\boldsymbol{\tau}} \ell = \mathbf{g}(\boldsymbol{\tau})$  w.r.t.  $\boldsymbol{\tau}$  is given. Let us consider  $\boldsymbol{\tau} = \boldsymbol{\phi}_{\boldsymbol{\tau}^{(\text{cur})}}(\boldsymbol{\eta}) = \mathbf{A}\mathbf{A}^T$ . By the chain rule, we have

$$\nabla_{\eta_{ij}} \ell = \text{Tr}(\mathbf{g}^T(\boldsymbol{\tau}) \nabla_{\eta_{ij}} \boldsymbol{\tau}) \Big|_{\boldsymbol{\eta}=\boldsymbol{\eta}_0} = \text{Tr}(\mathbf{g}^T(\boldsymbol{\tau}) \mathbf{A}^{(\text{cur})} \mathbf{E}_{ij} (\mathbf{A}^{(\text{cur})})^T),$$

so

$$\mathbf{g}(\boldsymbol{\eta}_0) = (\mathbf{A}^{(\text{cur})})^T \mathbf{g}(\boldsymbol{\tau}) \mathbf{A}^{(\text{cur})}. \quad (38)$$

Similarly, when  $\boldsymbol{\tau} = \mathbf{B}^{-T}\mathbf{B}^{-1}$ , we have

$$\nabla_{\eta_{ij}} \ell = \text{Tr}(\mathbf{g}^T(\boldsymbol{\tau}) \nabla_{\eta_{ij}} \boldsymbol{\tau}) \Big|_{\boldsymbol{\eta}=\boldsymbol{\eta}_0} = \text{Tr}(\mathbf{g}^T(\boldsymbol{\tau})(\mathbf{B}^{(\text{cur})})^{-T} \mathbf{E}_{ij} (\mathbf{B}^{(\text{cur})})^{-1}),$$

which gives

$$\mathbf{g}(\boldsymbol{\eta}_0) = (\mathbf{B}^{(\text{cur})})^{-1} \mathbf{g}(\boldsymbol{\tau}) (\mathbf{B}^{(\text{cur})})^{-T}. \quad (39)$$

### H.3. Simplification of Our Update

Consider the normal coordinate  $\phi_{\tau^{(\text{cur})}}(\boldsymbol{\eta}) = \mathbf{A}\mathbf{A}^T$ , where  $\boldsymbol{\eta}$  is symmetric, and  $\mathbf{A} := \mathbf{A}^{(\text{cur})} \text{Exp}(\frac{1}{2}\boldsymbol{\eta})$ .

We can compute the Euclidean gradient as  $\mathbf{g}(\boldsymbol{\eta}_0) = (\mathbf{A}^{(\text{cur})})^T \mathbf{g}(\boldsymbol{\tau}) \mathbf{A}^{(\text{cur})}$ .

Using the approximation in Eq. (9), we have

$$\mathbf{w}^{(\eta_1)} \leftarrow \mathbf{m}^{(\eta_0)}. \quad (40)$$

Since  $\boldsymbol{\eta}$  is symmetric, we can further show that the accurate approximation also gives the same update since the second dominant term vanishes as shown in Eq. (35).

By Eq. (31), the vector-Jacobian produce needed in Eq. (10) can be expressed as

$$\mathbf{w}^{(\xi_0)} = \mathbf{J}(\boldsymbol{\xi}_0) \mathbf{w}^{(\eta_1)} = \mathbf{w}^{(\eta_1)}. \quad (41)$$

Thus, we have  $\mathbf{w}^{(\xi_0)} = \mathbf{m}^{(\eta_0)}$ . As a consequence, our update (defined in Eq. (8)) can be simplified as below, where we can drop all the upper scripts and let  $\mathbf{w} = \mathbf{m}$ ,

$$\begin{aligned} \text{Momentum : } \mathbf{m} &\leftarrow \alpha \mathbf{m} + \beta \overbrace{(\mathbf{A}^{(\text{cur})})^T \mathbf{g}(\boldsymbol{\tau}) \mathbf{A}^{(\text{cur})}}^{=\mathbf{g}(\boldsymbol{\eta}_0)}, \\ \text{GD : } \boldsymbol{\eta}_1 &\leftarrow -\mathbf{m}, \\ \boldsymbol{\tau}^{(\text{new})} &\leftarrow \phi_{\tau^{(\text{cur})}}(\boldsymbol{\eta}_1) = \mathbf{A}^{(\text{cur})} \text{Exp}(\boldsymbol{\eta}_1) (\mathbf{A}^{(\text{cur})})^T \iff \mathbf{A}^{(\text{new})} \leftarrow \mathbf{A}^{(\text{cur})} \text{Exp}(\frac{1}{2}\boldsymbol{\eta}_1). \end{aligned} \quad (42)$$

Using Eq. (39), we also can obtain the following update if the normal coordinate  $\phi_{\tau^{(\text{cur})}}(\boldsymbol{\eta}) = \mathbf{B}^{-T}\mathbf{B}^{-1}$  is used, where  $\boldsymbol{\eta}$  is symmetric and  $\mathbf{B} := \mathbf{B}^{(\text{cur})} \text{Exp}(-\frac{1}{2}\boldsymbol{\eta})$ ,

$$\begin{aligned} \text{Momentum : } \mathbf{m} &\leftarrow \alpha \mathbf{m} + \beta \overbrace{(\mathbf{B}^{(\text{cur})})^{-1} \mathbf{g}(\boldsymbol{\tau}) (\mathbf{B}^{(\text{cur})})^{-T}}^{=\mathbf{g}(\boldsymbol{\eta}_0)}, \\ \text{GD : } \boldsymbol{\eta}_1 &\leftarrow -\mathbf{m}, \\ \boldsymbol{\tau}^{(\text{new})} &\leftarrow \phi_{\tau^{(\text{cur})}}(\boldsymbol{\eta}_1) = (\mathbf{B}^{(\text{cur})})^{-T} \text{Exp}(-\boldsymbol{\eta}_1) (\mathbf{B}^{(\text{cur})})^{-1} \iff \mathbf{B}^{(\text{new})} \leftarrow \mathbf{B}^{(\text{cur})} \text{Exp}(-\frac{1}{2}\boldsymbol{\eta}_1). \end{aligned} \quad (43)$$

## I. SPD Kronecker-product Submanifolds

We consider the following SPD submanifold.

$$\mathcal{M} = \left\{ \boldsymbol{\tau} = \mathbf{A}\mathbf{A}^T \in \mathcal{S}_{++}^{(pd) \times (pd)} \mid \mathbf{A} := \mathbf{K} \otimes \mathbf{C}, \mathbf{K} \in \mathbb{R}^{p \times p}, \mathbf{C} \in \mathbb{R}^{d \times d} \right\},$$

where  $\mathbf{U} = \mathbf{K}\mathbf{K}^T \succ 0$ ,  $\mathbf{W} = \mathbf{C}\mathbf{C}^T \succ 0$ , and both  $\mathbf{K}$  and  $\mathbf{C}$  are dense and non-singular.

### I.1. Blockwise Normal Coordinates

As mentioned in Sec. 4, we consider a block-diagonal approximation. For block  $\mathbf{K}$ , we consider the coordinate

$$\mathbf{A} = (\mathbf{K}^{(\text{cur})} \text{Exp}(\frac{1}{2\sqrt{d}}\boldsymbol{\eta}_K)) \otimes \mathbf{C}^{(\text{cur})},$$

where  $\boldsymbol{\eta}_K \in \mathbb{R}^{p \times p}$  is symmetric and  $\mathbf{A}^{(\text{cur})} = \mathbf{K}^{(\text{cur})} \otimes \mathbf{C}^{(\text{cur})}$ .

We show that the metric is trivialized at  $\boldsymbol{\eta}_K = \mathbf{0}$  under coordinate  $\boldsymbol{\eta}_K$ .

For notational simplicity, we let  $\mathbf{K}_0 = \mathbf{K}^{(\text{cur})}$ ,  $\mathbf{C}_0 = \mathbf{C}^{(\text{cur})}$ , and  $\boldsymbol{\tau}_0 = \boldsymbol{\tau}^{(\text{cur})}$ . Let  $\tilde{\boldsymbol{\eta}}_K$  denote the learnable part of  $\boldsymbol{\eta}_K$ .

By the Kronecker-product, we have  $\text{vec}^T(\mathbf{X})(\mathbf{U} \otimes \mathbf{W})\text{vec}(\mathbf{X}) = \text{vec}^T(\mathbf{X})\text{vec}(\mathbf{W}\mathbf{X}\mathbf{U}^T) = \text{Tr}(\mathbf{X}^T \mathbf{W}\mathbf{X}\mathbf{U}^T)$ , where  $\mathbf{x} := \text{vec}(\mathbf{X})$  and  $\mathbf{X} \in \mathbb{R}^{d \times p}$ .

By definition, the metric  $\mathbf{F}$  w.r.t. block  $\mathbf{K}$  in coordinate  $\boldsymbol{\eta}_K$  is

$$\begin{aligned} \mathbf{F}_K(\mathbf{0}) &= -2\mathbb{E}_{\mathcal{N}(\mathbf{0}, \boldsymbol{\tau})} \left[ \nabla_{\tilde{\boldsymbol{\eta}}_K}^2 \log \mathcal{N}(\mathbf{0}, \boldsymbol{\tau}) \right] \Big|_{\boldsymbol{\eta}_K = \mathbf{0}} \\ &= \mathbb{E}_{\mathcal{N}(\mathbf{x}|\mathbf{0}, \boldsymbol{\tau})} \left[ \nabla_{\tilde{\boldsymbol{\eta}}_K}^2 \left\{ \text{Tr}[\mathbf{x}^T (\mathbf{K}_0^{-T} \text{Exp}(\mathbf{0}) \mathbf{K}_0^{-1}) \otimes (\mathbf{C}_0^{-T} \mathbf{C}_0^{-1}) \mathbf{x}] \right\} \right] \Big|_{\boldsymbol{\eta}_K = \mathbf{0}} \quad (\text{drop the linear terms in the log-det term}) \\ &= \mathbb{E}_{\mathcal{N}(\mathbf{x}|\mathbf{0}, \boldsymbol{\tau})} \left[ \nabla_{\tilde{\boldsymbol{\eta}}_K}^2 \left\{ \text{Tr}[\mathbf{X}^T (\mathbf{C}_0^{-T} \mathbf{C}_0^{-1}) \mathbf{X} (\mathbf{K}_0^{-T} \text{Exp}(\mathbf{0}) \mathbf{K}_0^{-1}) \otimes \mathbf{I}] \right\} \right] \Big|_{\boldsymbol{\eta}_K = \mathbf{0}} \quad (\text{note: } \mathbb{E}_{\mathcal{N}(\mathbf{x}|\mathbf{0}, \boldsymbol{\tau}_0)}[\mathbf{X}^T (\mathbf{C}_0^{-T} \mathbf{C}_0^{-1}) \mathbf{X}] = d\mathbf{K}_0 \mathbf{K}_0^T) \\ &= d\mathbb{E}_{\mathcal{N}(\mathbf{x}|\mathbf{0}, \boldsymbol{\tau})} \left[ \nabla_{\tilde{\boldsymbol{\eta}}_E}^2 \left\{ \text{Tr}[\text{Exp}(\mathbf{0}) \boldsymbol{\eta}_E] \right\} \right] \Big|_{\boldsymbol{\eta}_K = \mathbf{0}}. \end{aligned} \quad (44)$$

It is easy to show that  $\mathbf{F}_K(\mathbf{0}) = \mathbf{I}$  w.r.t. block  $\mathbf{K}$  in coordinate  $\boldsymbol{\eta}_K$ , which means Assumption 2 holds.

Since block  $\mathbf{C}$  is frozen, we can prove as in Appx. H.1 that all assumptions are satisfied for the coordinate  $\boldsymbol{\eta}_K$ .

Similarly, for block  $\mathbf{C}$ , the coordinate  $\boldsymbol{\eta}_C$

$$\mathbf{A} = \mathbf{K}^{(\text{cur})} \otimes (\mathbf{C}^{(\text{cur})} \text{Exp}(\frac{1}{2\sqrt{p}} \boldsymbol{\eta}_C)),$$

where  $\boldsymbol{\eta}_C \in \mathbb{R}^{d \times d}$  is symmetric and  $\mathbf{A}^{(\text{cur})} = \mathbf{K}^{(\text{cur})} \otimes \mathbf{C}^{(\text{cur})}$ , defines a normal coordinate.

## I.2. (Euclidean) Gradient Computation for Deep Learning

We consider  $\boldsymbol{\tau} = \boldsymbol{\Sigma} = (\mathbf{K}\mathbf{K}^T) \otimes (\mathbf{C}\mathbf{C}^T)$ .

As suggested by Lin et al. (2021b), the Euclidean gradient w.r.t.  $\boldsymbol{\tau}$  is computed as  $\mathbf{g}_\Sigma := \frac{1}{2}(\nabla_{\boldsymbol{\mu}}^2 \ell(\boldsymbol{\mu}) - \boldsymbol{\Sigma}^{-1})$ .

In KFAC (Martens & Grosse, 2015), the Hessian is approximation as  $\nabla_{\boldsymbol{\mu}}^2 \ell(\boldsymbol{\mu}) \approx \boldsymbol{\mu}_{AA} \otimes \boldsymbol{\mu}_{GG}$ , where matrices  $\boldsymbol{\mu}_{AA} \in \mathbb{R}^{p \times p}$  and  $\boldsymbol{\mu}_{GG} \in \mathbb{R}^{d \times d}$  are two dense symmetric positive semi-definite matrices and are computed as suggested by the authors.

To handle the non-singularity of  $\boldsymbol{\mu}_{AA}$  and  $\boldsymbol{\mu}_{GG}$ , Martens & Grosse (2015) introduce a damping term  $\lambda$  when it comes to inverting  $\boldsymbol{\mu}_{AA}$  and  $\boldsymbol{\mu}_{GG}$  such as  $\boldsymbol{\mu}_{AA}^{-1} \approx (\boldsymbol{\mu}_{AA} + \lambda \mathbf{I}_p)^{-1}$  and  $\boldsymbol{\mu}_{GG}^{-1} \approx (\boldsymbol{\mu}_{GG} + \lambda \mathbf{I}_d)^{-1}$ .

In our update, we use the KFAC approach to approximate the Hessian. We add a damping term by including it in  $\mathbf{g}_\Sigma$  as

$$\mathbf{g}_\Sigma \approx \frac{1}{2} \underbrace{(\boldsymbol{\mu}_{AA} \otimes \boldsymbol{\mu}_{GG} + \lambda \mathbf{I}_{pd})}_{\approx \nabla_{\boldsymbol{\mu}}^2 \ell(\boldsymbol{\mu})} - \boldsymbol{\Sigma}^{-1},$$

where  $\mathbf{I}_{pd} = \mathbf{I}_p \otimes \mathbf{I}_d$  and  $\boldsymbol{\Sigma}^{-1} = (\mathbf{K}^{-T} \mathbf{K}^{-1}) \otimes (\mathbf{C}^{-T} \mathbf{C}^{-1})$ .

The Euclidean gradient  $\mathbf{g}(\boldsymbol{\eta}_{K_0})$  w.r.t.  $\boldsymbol{\eta}_E$  can be computed as

$$\frac{\partial \ell}{\partial \boldsymbol{\eta}_{K_{ij}}} = \text{Tr} \left( \left( \frac{\partial \ell}{\partial \boldsymbol{\tau}} \right)^T \frac{\partial \boldsymbol{\tau}}{\partial \boldsymbol{\eta}_{K_{ij}}} \right) = \text{Tr} \left( [\mathbf{g}_\Sigma]^T \frac{\partial \boldsymbol{\tau}}{\partial \boldsymbol{\eta}_{K_{ij}}} \right).$$

There are three terms in the Euclidean gradient w.r.t.  $\boldsymbol{\tau} = \boldsymbol{\Sigma}$ :

$$\mathbf{g}_\Sigma \approx \frac{1}{2} (\boldsymbol{\mu}_{AA} \otimes \boldsymbol{\mu}_{GG} + \lambda \mathbf{I}_p \otimes \mathbf{I}_d - (\mathbf{K}^{-T} \mathbf{K}^{-1}) \otimes (\mathbf{C}^{-T} \mathbf{C}^{-1})).$$

Thus, the Euclidean gradient w.r.t.  $\boldsymbol{\eta}$  can be expressed as three parts. For notational simplicity, we let  $\mathbf{K}_0 = \mathbf{K}^{(\text{cur})}$ ,  $\mathbf{C}_0 = \mathbf{C}^{(\text{cur})}$ , and  $\boldsymbol{\tau}_0 = \boldsymbol{\tau}^{(\text{cur})}$ .

The first part of  $\frac{\partial \ell}{\partial \eta_{K_{ij}}}$  can be computed via

$$\begin{aligned} \frac{1}{2} \text{Tr}([\boldsymbol{\mu}_{AA} \otimes \boldsymbol{\mu}_{GG}]^T \frac{\partial \boldsymbol{\tau}}{\partial \eta_{K_{ij}}}) &= \frac{1}{2\sqrt{d}} \text{Tr}[(\boldsymbol{\mu}_{AA}^T \mathbf{K}_0 \mathbf{E}_{ij} \mathbf{K}_0^T) \otimes (\boldsymbol{\mu}_{GG}^T \mathbf{C}_0 \mathbf{C}_0^T)] \\ &= \frac{1}{2\sqrt{d}} \text{Tr}(\boldsymbol{\mu}_{GG}^T \mathbf{C}_0 \mathbf{C}_0^T) \text{Tr}(\boldsymbol{\mu}_{AA}^T \mathbf{K}_0 \mathbf{E}_{ij} \mathbf{K}_0^T). \end{aligned}$$

We obtain the expression for the first part of  $\frac{\partial \ell}{\partial \eta_K}$  as  $\frac{1}{2\sqrt{d}} \text{Tr}(\mathbf{C}_0^T \boldsymbol{\mu}_{GG} \mathbf{C}_0) \mathbf{K}_0^T \boldsymbol{\mu}_{AA} \mathbf{K}_0$ .

Similarly, we can obtain the second and third parts, which gives altogether the Euclidean gradient  $\mathbf{g}(\boldsymbol{\eta}_K)$  via

$$\mathbf{g}(\boldsymbol{\eta}_{K_0}) = \frac{1}{2\sqrt{d}} [\text{Tr}(\mathbf{C}_0^T \boldsymbol{\mu}_{GG} \mathbf{C}_0) \mathbf{K}_0^T \boldsymbol{\mu}_{AA} \mathbf{K}_0 + \lambda \text{Tr}(\mathbf{C}_0^T \mathbf{C}_0) \mathbf{K}_0^T \mathbf{K}_0 - d \mathbf{I}_p]. \quad (45)$$

Likewise, the Euclidean gradient  $\mathbf{g}(\boldsymbol{\eta}_C)$  is

$$\mathbf{g}(\boldsymbol{\eta}_{C_0}) = \frac{1}{2\sqrt{p}} [\text{Tr}(\mathbf{K}_0^T \boldsymbol{\mu}_{AA} \mathbf{K}_0) \mathbf{C}_0^T \boldsymbol{\mu}_{GG} \mathbf{C}_0 + \lambda \text{Tr}(\mathbf{K}_0^T \mathbf{K}_0) \mathbf{C}_0^T \mathbf{C}_0 - p \mathbf{I}_d]. \quad (46)$$

### I.3. Derivation of the Update

We consider the update for block  $\boldsymbol{\eta}_K$ . By the approximation in Eq. (9), we have

$$\mathbf{w}^{(\eta_{K_1})} \leftarrow \mathbf{m}^{(\eta_{K_0})}, \quad (47)$$

for block  $\boldsymbol{\eta}_K$ . Since  $\boldsymbol{\eta}_K$  is symmetric, we can further show that the accurate approximation also gives the same update since the second dominant term vanishes as shown in Eq. (35).

Since  $\boldsymbol{\eta}_K$  is symmetric (see Eq. (31)), the vector-Jacobian produce needed in Eq. (10) can be expressed as

$$\mathbf{w}^{(\xi_{K_0})} = \mathbf{J}(\boldsymbol{\xi}_{K_0}) \mathbf{w}^{(\eta_{K_1})} = \mathbf{w}^{(\eta_{K_1})}. \quad (48)$$

Thus, we have  $\mathbf{w}^{(\xi_{K_0})} = \mathbf{m}^{(\eta_{K_0})}$  for  $\boldsymbol{\eta}_K$ . As a consequence (similar to Appx. H.3), our update (defined in Eq. (8)) to update block  $\boldsymbol{\eta}_K$  can be expressed as below, where we drop all upper scripts and let  $\mathbf{w} = \mathbf{m}$ ,

$$\begin{aligned} \text{Momentum} : \mathbf{m}_K &\leftarrow \alpha \mathbf{m}_K + \beta \mathbf{g}(\boldsymbol{\eta}_{K_0}), \\ \text{GD} : \boldsymbol{\eta}_{K_1} &\leftarrow -\mathbf{m}_K, \\ \mathbf{K} &\leftarrow \mathbf{K}^{(\text{cur})} \text{Expn}\left(\frac{1}{2\sqrt{d}} \boldsymbol{\eta}_{K_1}\right). \end{aligned} \quad (49)$$

Note that the affine-invariant metric is defined as twice of the Fisher-Rao metric. To recover structured NGD, we have to set our step-size  $\beta$  to twice as the step-size of structured NGD. Letting  $\beta = 2\beta_2$ , we can reexpress the above update for block  $\boldsymbol{\eta}_K$  as

$$\begin{aligned} \mathbf{m}_K &\leftarrow \alpha \mathbf{m}_K + \frac{\beta_2}{\sqrt{d}} \mathbf{g}(\boldsymbol{\eta}_{K_0}), \\ \mathbf{K} &\leftarrow \mathbf{K}^{(\text{cur})} \text{Expn}(-\mathbf{m}_K). \end{aligned}$$

A similar update for the block  $\boldsymbol{\eta}_C$  can also be obtained.